REPORT DOCUMENTATION PAGE

Form Approved
OMB No. 074-0188

1. AGENCY USE ONLY (Leave blank)	2. REPORT DATE	3. REPORT TYPE AND DATES COVERED
	1995	Final Technical Report, 1995

4. TITLE AND SUBTITLE
Initial Arctic Acoustic Source Design Study

5. FUNDING NUMBERS
Subcontract No. 31-960019-94

6. AUTHOR(S)
M.M. Slavinsky, B. Bogolubov, A. Virovlyansky, et al.

7. PERFORMING ORGANIZATION NAME(S) AND ADDRESS(ES)
Advanced Science & Technology Centre
"GRAN"

8. PERFORMING ORGANIZATION REPORT NUMBER
N/A

9. SPONSORING / MONITORING AGENCY NAME(S) AND ADDRESS(ES)
SERDP
901 North Stuart St. Suite 303
Arlington, VA 22203

10. SPONSORING / MONITORING AGENCY REPORT NUMBER
N/A

11. SUPPLEMENTARY NOTES
Final Technical Report written for the Advanced Science & Technology Centre, Nizhny Novgorod, Russia, 1995. This work was supported in part by Subcontract No. 31-960019-94. The United States Government has a royalty-free license throughout the world in all copyrightable material contained herein. All other rights are reserved by the copyright owner.

12a. DISTRIBUTION / AVAILABILITY STATEMENT
Approved for public release: distribution is unlimited

12b. DISTRIBUTION CODE
A

13. ABSTRACT ***(Maximum 200 Words)***

The first pilot experiment on transarctic underice low-frequency (LF) sound propagation in Arctic Ocean-Transarctic Acoustic Propagation (TAP) experiment was successfully carried out in April, 1994. This experiment was performed by American, Canadian and Russian scientists. The acoustic data provided by tone and complex signals propagation along paths of lengths~900 km and ~2600 km were collected within 5 days. The TAP experiment has confirmed the principle possibility of observing rather low temperature water-mass trends and averaged over Arctic ice cover characteristics provided by long-term observation of variable phase, propagation time and amplitude of acoustic signals.

Acoustic monitoring of climatic variations and study of temperature noises caused by space-time variability of dynamic processes in the Arctic Ocean will require the arrangement of an acoustic network capable of at least ten year functioning. The new program - Arctic Climate Observations using Underwater Sound (ACOUS) being developed for these purposes implies at the first stage arranging continuous collection of acoustic data on paths similar to TAP experiment during 1996-1997.

14. SUBJECT TERMS
SERDP, low-frequency sound propagation, , Transarctic Acoustic Propagation, ACOUS

15. NUMBER OF PAGES
62

16. PRICE CODE
N/A

17. SECURITY CLASSIFICATION OF REPORT	18. SECURITY CLASSIFICATION OF THIS PAGE	19. SECURITY CLASSIFICATION OF ABSTRACT	20. LIMITATION OF ABSTRACT
unclass.	unclass.	unclass.	UL

ADVANCED SCIENCE & TECHNOLOGY CENTRE
"GRAN"

Subcontract No. 31-960019-94

INITIAL ARCTIC ACOUSTIC SOURCE DESIGN STUDY

FINAL TECHNICAL REPORT

Mark Slavinsky, Boris Bogolubov, Anatoly Virovlyansky

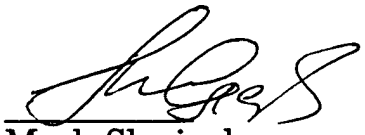

Mark Slavinsky
Principal Investigator

Nizhny Novgorod, Russia, 1995

The work has been fulfiled by:

Barashkov A. D.

Bogolubov B. N.

Virovljansky A. L.

Vorobjev V. G.

Dubovoj Ju. A.

Pigalov K. E.

Sizmin A. M.

Slavinsky M. M.

Smirnov S. Ju.

Fokin V. N.

Shepkin K. E.

Translated by -Rudik N.V.

Table of Contents

1. INTRODUCTION

The first pilot experiment on transarctic underice low-frequency (LF) sound propagation in Arctic Ocean - Transarctic Acoustic Propagation (TAP) experiment was succesfully carried out in April, 1994. This experiment was performed by American, Canadian and Russian scientists. The acoustic data provided by tone and complex signals propagation along paths of lengths ~ 900 km and ~ 2600 km were collected within 5 days. The TAP experiment has confirmed the principal possibility of observing rather low temperature water-mass trends and averaged over Arctic ice cover characteristics provided by long-term observation of variable phase, propagation time and amplitude of acoustic signals [1,2].

Acoustic monitoring of climatic variations and study of temperature noises caused by space-time variability of dynamic processes in the Arctic Ocean will require the arrangement of an acoustic network capable of at least ten year functioning. The new program - Arctic Climate Observations using Underwater Sound (ACOUS) being developed for these purposes implies at the first stage arranging continuous collection of acoustic data on paths similar to TAP experiment during 1996-1997.

One of the key elements of this long-term Program is the creation of reliable emitting and receiving complexes capable of functioning within several years. The development of such systems operating under the conditions of a complicated ice situation demands the application of new approaches to solve occurred problems. Thus, for a receiving antenna using thin opticfiber cables, the possibility is considered to use the technology of down-the-hole drilling for laying the cable without its contact with ice cover when it reaches the coast. Emitting systems employing, as a rule, higher-power signals and, consequently, thicker cable lines requires, evidently, some other approaches at the present stage.

The present report deals with potential ways of creating a LF acoustic Emitting Complex (EC) serving as a basis for step-by-step development of Acoustic Thermometry network in the Arctic Ocean in 1996-1997 and later.

2. MAIN REQUIREMENTS TO EMITTING COMPLEX CHARACTERISTICS

2.1. ANALISIS OF SPECIFIC EMPLOYMENT OF EMITTING COMPLEX IN THE ARCTIC

The TAP experiment has demonstrated that the 20 Hz emission frequency enables one to insure the necessary measurement quality at a path about 2600 km long for the acoustic radiation level 195 dB. At the same time at paths of the order of 900 km one can obviously provide satisfactory measurements at the radiation level of 175 dB at the frequency of 20 Hz and at the level of 185 dB at the frequency 30 Hz. It should be noted that these estimates correspond to small (less than 100 m) submersion depth of the source in the underwater sound channel of the Arctic type. To effectively drive the lower modes which are most sensitive to variation of the water mass temperature and the ice cover characteristics, the source should be placed at a depth of 100-150 m. At the same time, to realize high potential sensitivity of the acoustic thermometry in the Arctic regions demonstrated within the TAP experiment, the steady state of the complex must be provided.

Taking into account possible deployment of the emitting complex and the character of the bottom relief in the east Arctic sector, it seems to be proper at the first stage of realizing the ACOUS program to deploy the emitting complex in the shelf zone in the region of the Spitsbergen archipelago or the Franz Josef Land with depths of 400-600 m. The place of deployment should be chosen maximally close to the transition of the shelf to the region of the continental boderland slope. This will permit, on the one hand, to avoid additional loss caused by

bottom absorbtion and scattering of sound in the shelf zone. On the other hand, small length of cable from the bottom to the moored source at low current velocities typical of the Arctic will enable one to decrease the horizontal and vertical displacements of the source from the "middle" point to admissible values. This is of special importance, since at proper limiting displacements of the source the necessity disappears to transmit current coordinates of the source in real or (quasi-real) time scale during each emission session. Due to long-term functioning and practically impossible repairement in the Arctic the emitting complex reliability becomes the governing factor. And first of all, it is necessary to solve the problem of conserving the cable line in the place of its reaching the coast under the conditions of the variable ice situation (Fig.1).

The consideration of the set of the mentioned factors indicates that occurred numerous problems can be best solved by creating an autonomous moored emitting complex. Direct contact of the complex equipment and the ice cover is prevented in this case. This complex will not require laying an expensive and unreliable cable line and arranging a long-term coast station for servicing the complex. Besides, when there is no cable communication of the complex with the coast, the place of its deployment can be rather free chosen. The problem of providing high time stability of emission parameters and regimes during the entire period of functioning, occurred in the autonomous complex is solved by using economic schemes designed for correcting the time scale of the high-accuracy frequency and time standards. To insure the measurement accuracy of the delay time of the order of a millisecond, the relative instability of the time scale of the complex within a year is to be of the order of 10^{-11}.

The capability of realizing the autonomous emitting complex depends on the potential of autonomous energy sources, the

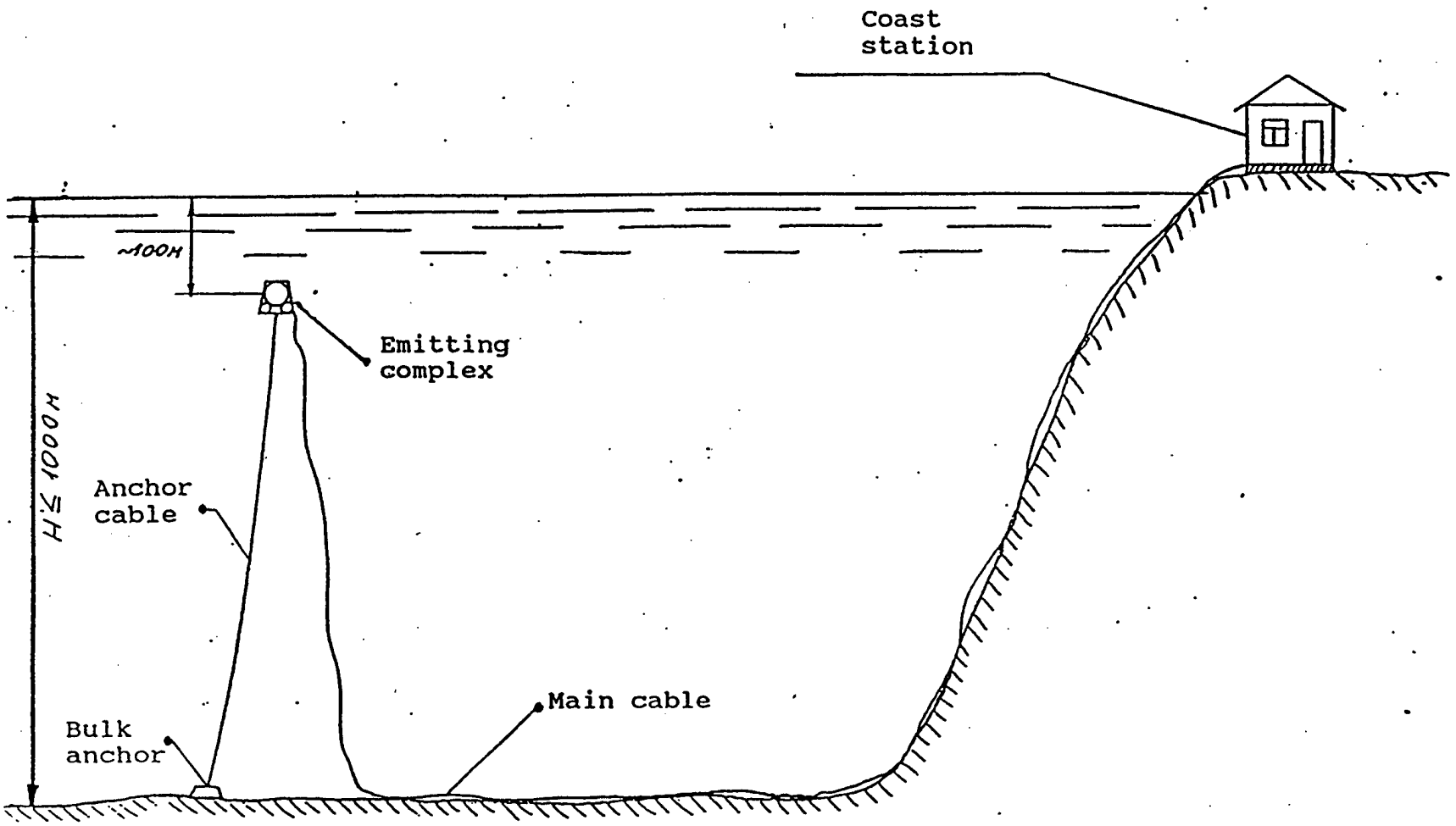

Fig.1. Emitting complex, moored cable variant. Coast station and main cable are absent in the autonomous emitting complex variant.

emitting complex efficiency and on the type of emitting signals and time regimes of their radiation.

2.2. EMITTED SIGNAL CHARACTERISTICS

In the acoustic thermometry in the Arctic, at least two types of emitted signals can succesfully be used. Narrowband continuous sine wave tone (CW) are used to measure variation in phase and time of signal propagation. Pulse signals with complex modulation, for example, maximal length sequences (MLS) having sharp correlation function can be employed after cross-correlation processing for measuring time variations of signal arrival time transmitted by individual time-resolved modes. It should be noted that the use of CW signals for the same aims requires space selection of mode signals provided by space distributed antennas. At the same time, MLS signals processed by an individual hydrophone can also store information on the variation of amplitude-phase signal characteristics at the carrier frequency. However, together with these advantages MLS signals require large energy consumption for emission, since the "average" efficiency of resonance sources in the frequency band occupied by MLS signals may prove to be essentially lower than that at the resonance frequency of emitted CW signals. As a consequence, when estimating the emitting complex parameters, we shall use the "worst" energy situation, i.e. the case of emitting MLS signals in the necessary frequency band.

Let us consider now the problem on choosing the frequency band or the duration of a compressed MLS signal recorded by an individual hydrophone. We deal here with the mode resolution by their arrival times. The problem of ray resolution is not considered here, since in experiemnt with carrier frequencies of the order of 10 - 30 Hz being optimum from the viewpoint of transmission loss minimization for propagation in the Arctic [3], the interpretation of the obtained data in terms of the ray approach is rather problematic. On the other hand, the practical

realizability of mode resolution at the transarctic paths, by employing a point source, has been demonstrated within the TAP experiment [2]. The results presented below are based on the conclusions of paper [4] devoted to the analysis of the mode structure of signals at long distances in ocean waveguides.

Let us introduce some designations. We consider a range-independent waveguide with a refraction index profile c(z), where z is the vertical coordinate. For definiteness we shall deal with the upward refracting sound speed profile typical of the Arctic, an example of which is depicted in fig.2. Let c_0 be the sound speed near the surface (z = 0). We assume that the point source exciting a field emits a pulse signal of duration τ_0 at the carrier frequency F. The bandwidth of this signal is $\Delta F=1/\tau_0$. Each mode will be characterized either by its number m, or by the grazing angle χ at which its Brillouin waves (at the central frequency F) fall on the upper boundary z = 0.

The pulse sound signal in an acoustic waveguide can be treated as the superposition of pulses carried by separate modes. To find out the conditions under which such pulses reach the reception point without overlapping (this is the condition of mode resolution), the influence of two competing factors should be compared: the pulse travel difference caused by different group velocities of modes and the spread of these pulses due to wave dispersion. Such an investigation has been carried out in Ref.[4], the main results of which (all of them are obtained in the frames of the WKB approximation) are as follows.

At a rather long distance the pulse carried by the m-th mode can be resolved under the condition fulfillment:

$$mT > \tau_0 \qquad (1)$$

where T = 1/F is the carrier frequency period. This result is obtained for the modes, whose lower turning points lie in the water bulk (i.e. for the modes not interacting with the bottom) and remains valid irrespective of specific shape of the sound speed profile. The allowance for the finite length of the acoustic path imposes, however, an additional limitation which is already dependent on the sound speed profile and is expressed by the inequality

$$\frac{\tau_0}{mT} < \frac{r}{L(\chi_m)}, \qquad (2)$$

where r is the distance to the observation point, χ_m is the grazing angle of the Brillouin wave of the m-th mode,

$$L(\chi_m) = \frac{\lambda D^3(\chi_m)}{\left|\frac{dD}{d\chi}\right|_{\chi=\chi_m}},$$

$\lambda = c_0/F$ is the wavelength, $D(\chi)$ is the dependence of the ray cycle length on its grazing angle χ near the surface. In this case the value τ_0/mT at such long ranges, where $r >> L(\chi_m)$, shows the ratio of the difference of arrival times of this pulse and the pulse carried by the (m+1)-th mode and the duration of the pulse carried by the m-th mode and. In other words, the τ_0/mT ratio yields the resolution quality of the m-th mode at very long ranges.

The conditions (1) and (2) imply the estimate of the admissible duration range of the emitted pulse

$$mT < \tau_0 < \frac{rmT}{L(\chi_m)} \qquad (3)$$

for which the m-th mode resolution is achieved at the distance r. As is mentioned above, it has been obtained in the WKB approximation and, thus, its applicability range is, strictly speaking, limited by the case of high frequencies and modes of rather high numbers. Nevertheless our numerical calculations performed for several waveguides with the sound speed profiles typical for the Arctic, have demonstrated that this ratio enables one to draw quantitative conclusions on the possibility of resolution of even first several modes when operating at frequencies of the order of a few tens of Hz. Numerical calculations performed to compute pulse signals emitted by a point source and received at the distances of 900 and 2600 km were carried out using a mode code. The numbers of modes resolved by their arrival times were compared with the estimations of the numbers of such modes obtained from the criterion (3).

As an example we present the results of the calculations carried out for a waveguide with the sound speed profile shown in fig.2. The carrier frequency F was taken equal to 20 Hz, while the source and receiver depths amounted to 150 m. In calculations we have taken into account only the contributions of those modes the lower turning points of which are rather far from the bottom (the modes with turning points at depths not exceeding 2.5 km were taken). There are 6 such modes at a frequency of 20 Hz in this waveguide.

According to the criterion (1) for the resolution of all 6 modes the emitted signal duration τ_0 should not exceed 0.3 s, i.e. the frequency band ΔF should not be larger than 3 Hz. But additional restrictions are implied here by the condition (2). Figure 3 deals with the dependence $L(\chi)$ (the angle χ is expressed in degrees) for the waveguide, the values $L(\chi_m)$ corresponding to the 6 analyzed modes being marked with points.

Since due to the peculiarities of the profile shape of the sound speed in the Arctic, the pulse carried by the first mode arrives significantly later than all the rest and is practically always well resolved, we have paid attention to the determination of the resolution conditions for the modes with numbers 2,...,6. The time dependences of signals received at a distance of 2600 km for τ_0 varying from 0.125 s (ΔF = 8 Hz) to 0.5 s (ΔF = 2 Hz) are shown in figs. 4 - 7. Only those parts of the received pulse are shown in these figures, which are formed by the contributions of modes with numbers 2,...,6. The pulse carried by the first mode arrives at the time instant t = 1800 s and is not shown in the figures. The number of the corresponding mode is shown near every resolved pulse. At such a long distance the right-hand side of inequality (3) does not introduce any limitations. Therefore, the resolution possibility is fully determined by the left-hand side (i.e. by inequality (1)). According to this condition, the number of resolved modes varies from two for τ_0 = 0.125 s (ΔF = 8 Hz) to six for $\tau_0 > 0.25$ s ($\Delta F < 4$ Hz).

At shorter distances the allowance for the right-hand side of inequality (3) already leads to considerable restrictions, which is also confirmed by our numerical calculations. In particular, the shape of a signal with τ_0 = 0.5 s (ΔF = 2 Hz) received at a distance of 900 km is displayed in fig.8. Only 4 modes are resolved here, which corresponds to the criterion (3).

The functions $L(\chi)$ employed by us for estimates significantly depend on specific profile of the sound speed. In particular, for the sound speed profile given in fig.9 measured at the emission point within the TAP experiment, the values $L(\chi_m)$ (see fig.10) markedly differ from the analogous values calculated for the profile shown in fig.2. The restrictions imposed by the right-hand side of the inequality (3) are revealed here at much longer distances. Thus, for example, when operating at the central frequency F = 20 Hz at a distance of 2600 km, it is impossible according to the criterion (3) at any choice of the frequency band ΔF of the emitted signal, to resolve by arrival times more than 3 - 4 first modes. This prediction (made without taking account of the sound speed profile variations along the path) agrees with the results of the numerical simulation and the experimental data given in [2].

All the calculations and qualitative estimates are referred to the case when the central frequency equaled 20 Hz. When passingover to the central frequency 30 Hz the mode resolution conditions yielded by (3) vary insignificantly. For the mode with the assigned number, the left inequality boundary decreases by 30%. The right boundary variation is, as a rule, even less, since it occurs only because of the angle χ_m variation.

Taking into account all the said above, the following conclusions can be drawn. To resove modes by their arrival times, one should not essentially reduce the emitted pulse duration (one should not tend to very wide broadening of its frequency band). There is a finite interval of the emitted signal durations, for which the given mode can be resolved. This interval can be estimated using the relationship (3). In accordance with our calculations for several typical sound speed profiles, when operating at the frequencies 20-30 Hz the increase of the source bandwidth by 3-4 Hz does not result in the mode resolution improvement when reception is provided by a single hydrophone.

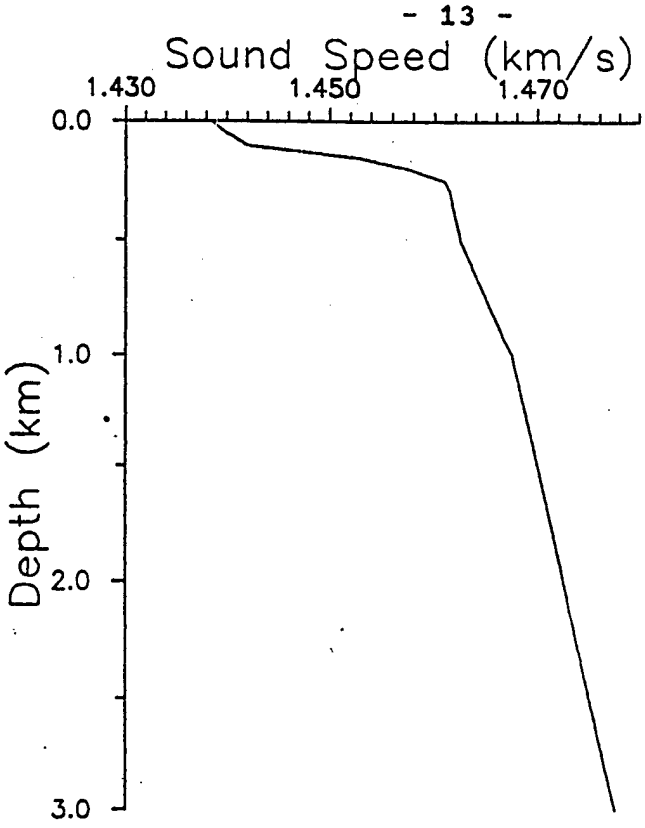

Fig.2. Example of typical profile of sound speed in the Arctic.

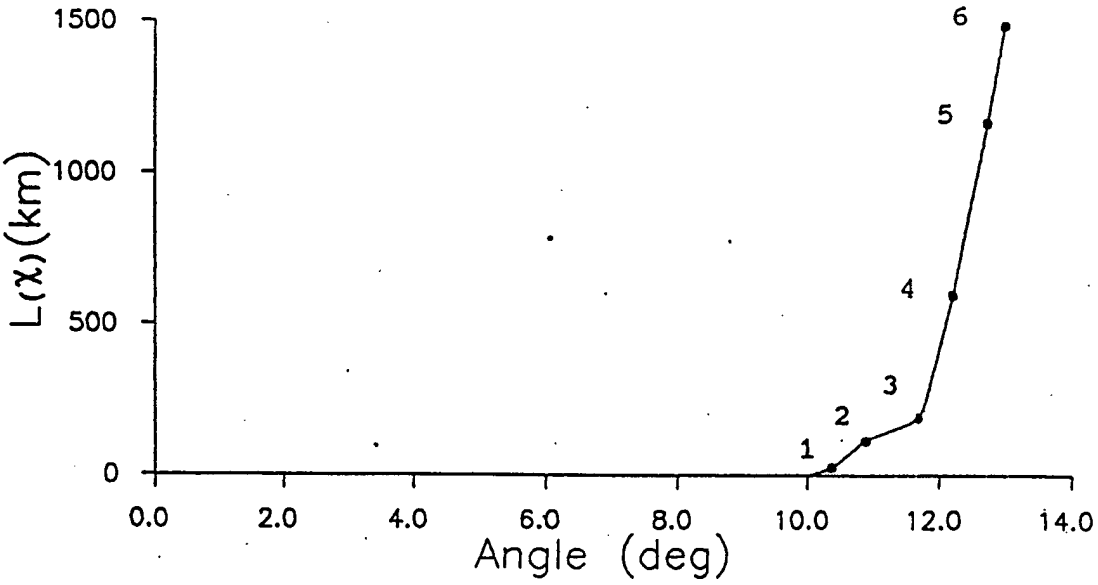

Fig.3. Dependence L(χ) for sound speed profile shown in fig.2.

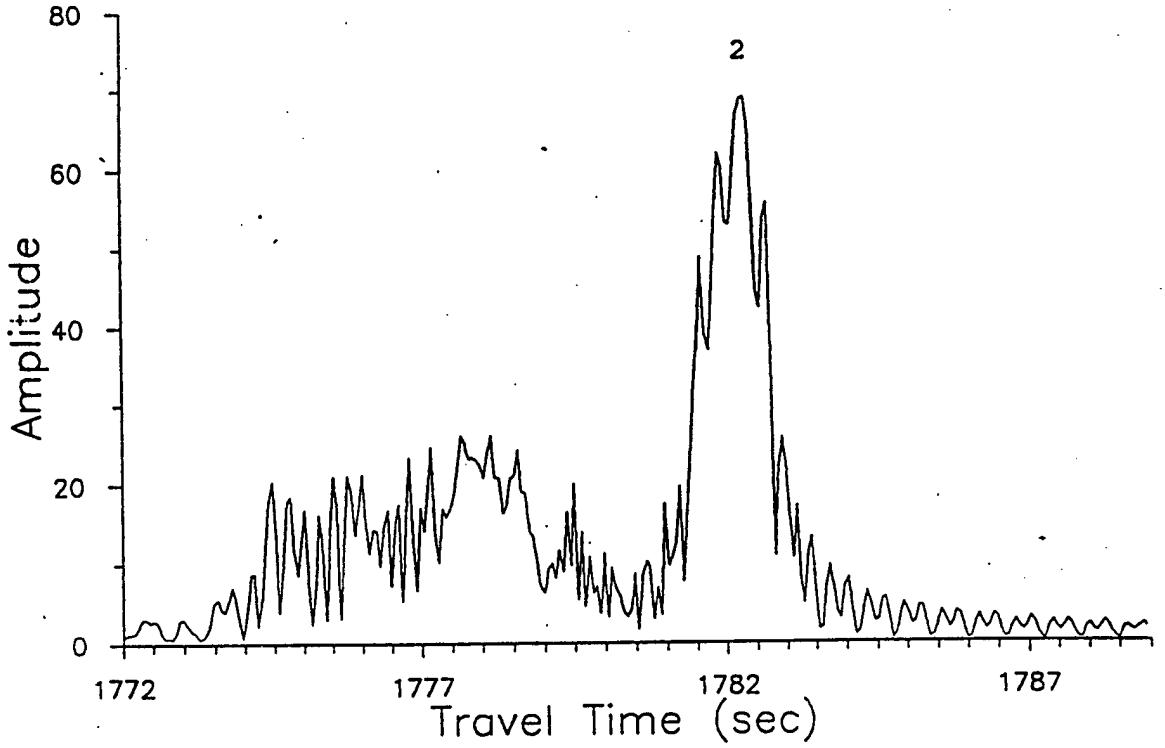

Fig.4. Signal part formed by contributions of 2 - 6 modes at distance 2600 km long in waveguide with sound speed profile given in fig.2. (Central frequency of emitted signal F = 20 Hz, emitted signal duration τ_0 = 0.125 s (ΔF = 8 Hz).

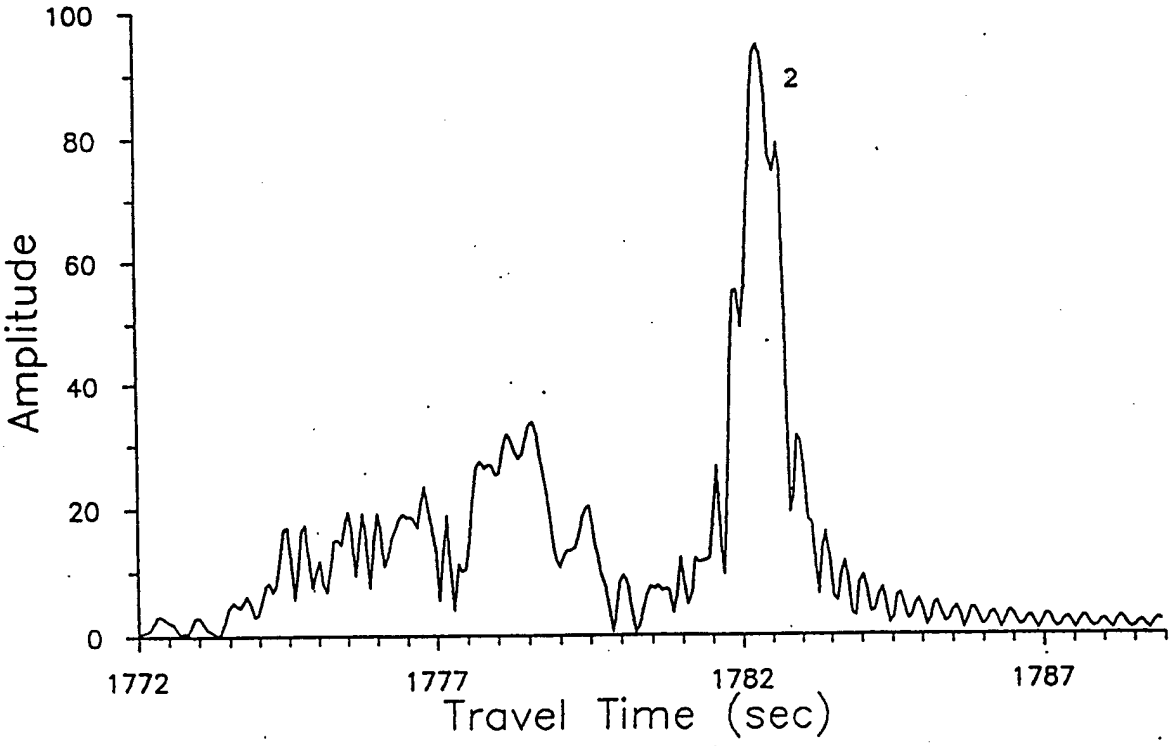

Fig.5. The same for τ_0 = 0.2 s (ΔF = 5 Hz).

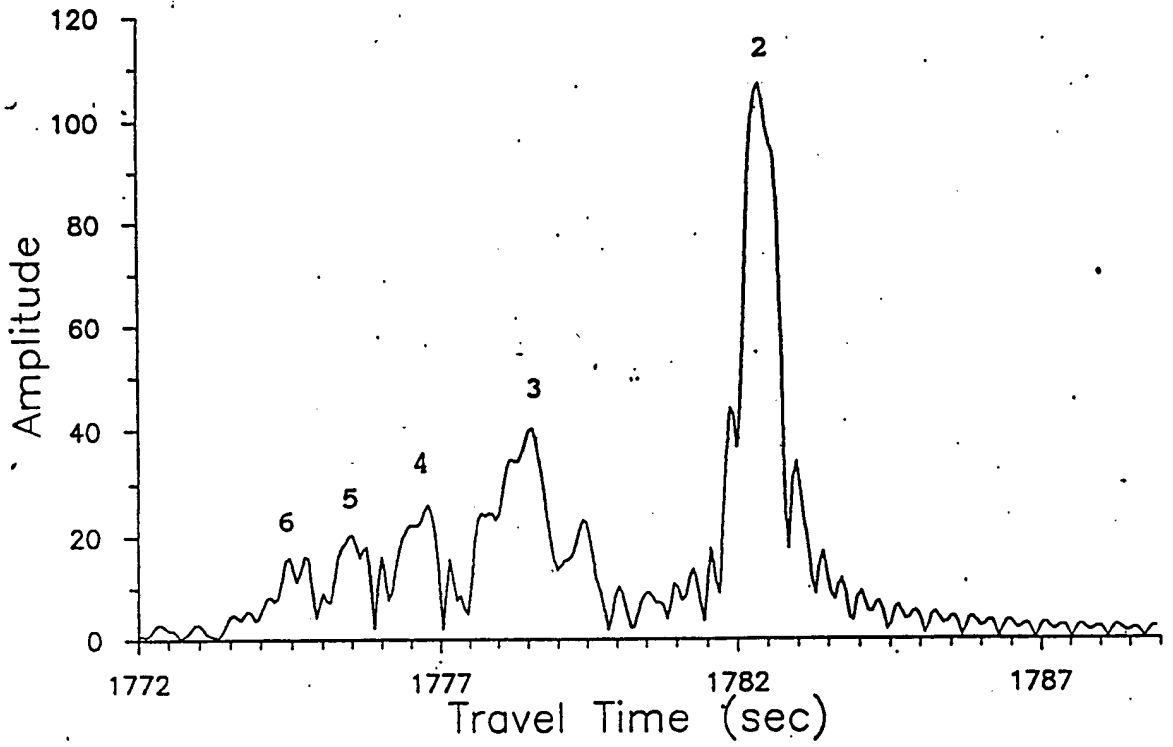

Fig.6. The same for τ_0 = 0.25 s (ΔF = 4 Hz).

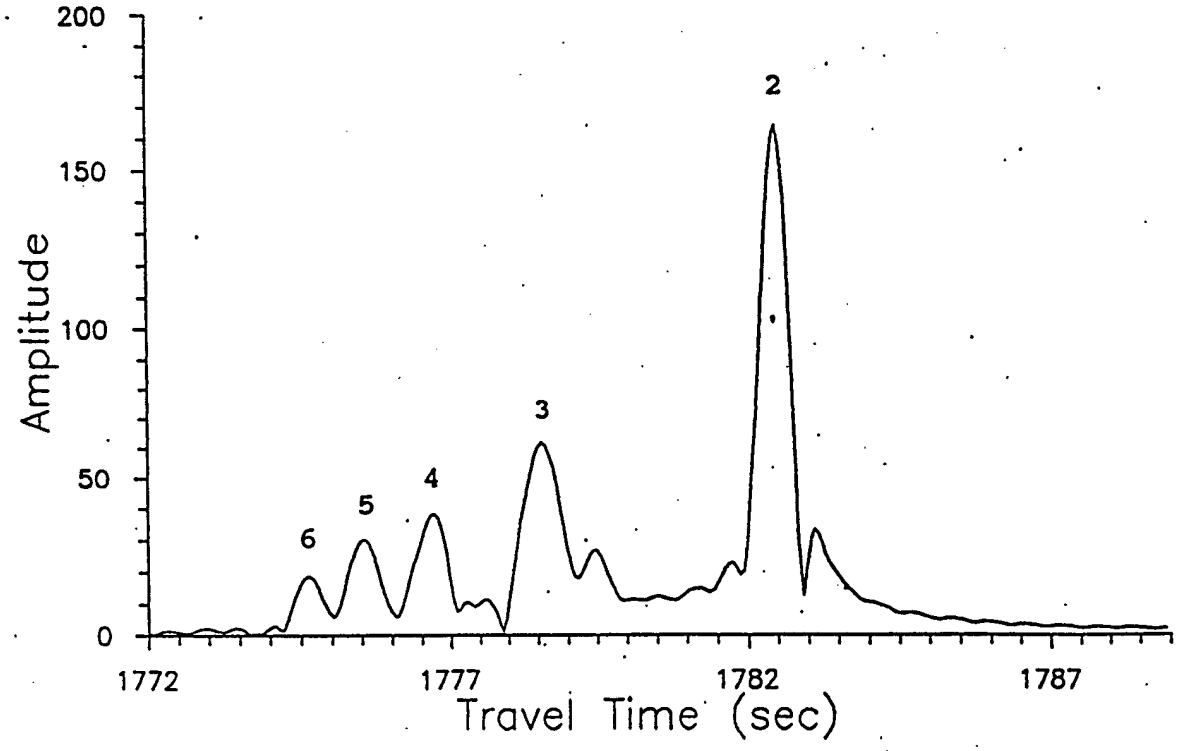

Fig.7. The same for τ_0 = 0.05 s (ΔF = 2 Hz).

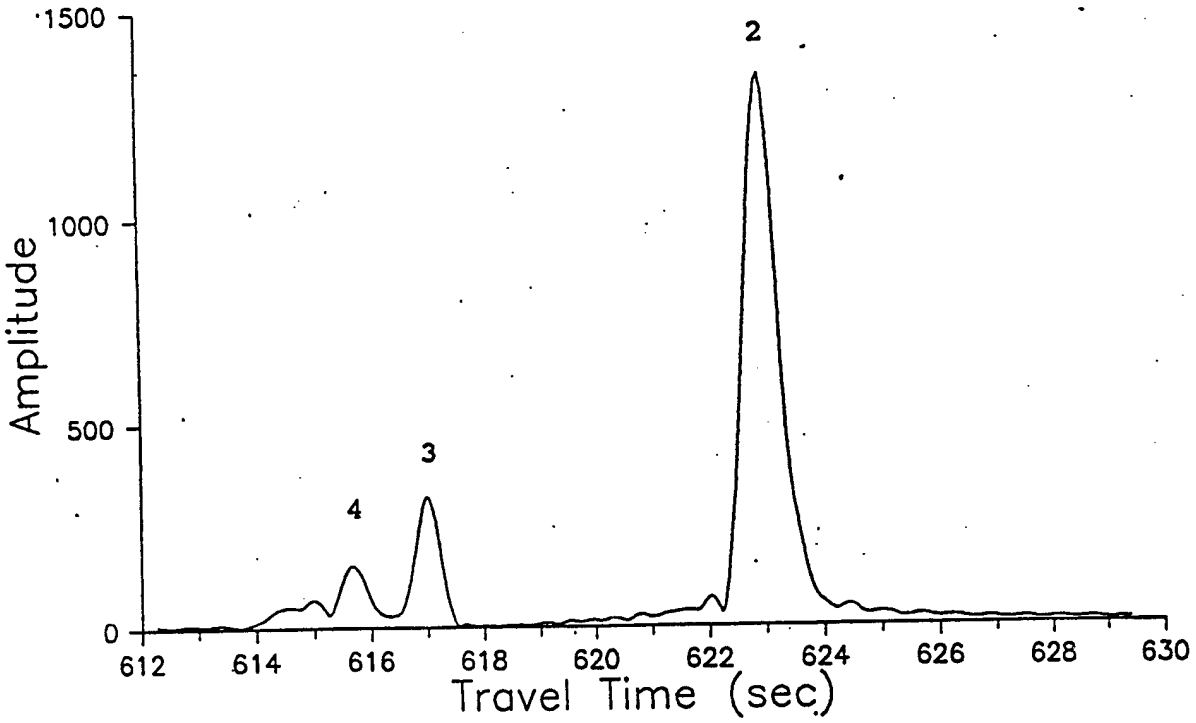

Fig.8. Signal at distance of 9.00 km in waveguide with sound speed profile displayed in fig.2. Central frequency of emitted signal F = 20 Hz,
emitted signal duration τ_0 = 0.5 s (ΔF = 2 Hz)

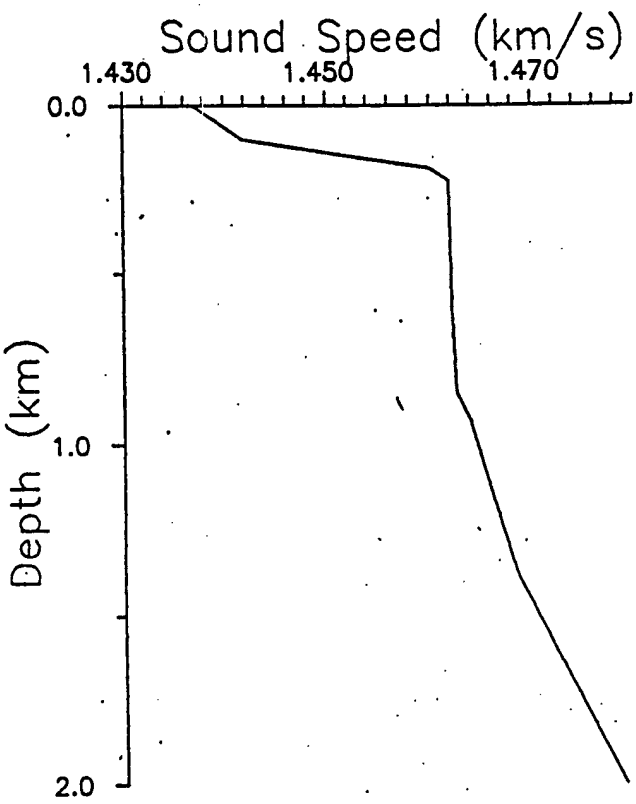

Fig.9. Sound speed profile at source deployment place in TAP experiment.

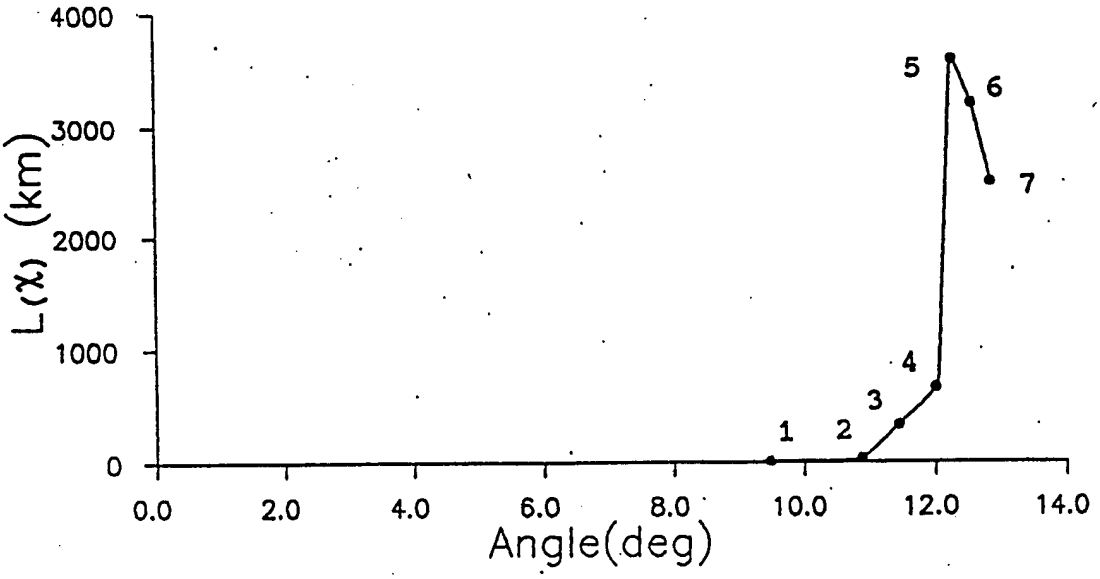

Fig.10. Dependence L(χ) for sound speed profile depicted in fig.9.

The problem on choosing the duration τ and the repetition rate T of emission sessions is not of less importance than that of determining the frequency band of emitted signals. These parameters should, in principle, be selected based on the condition of minimizing the estimate variance of average time of acoustic pulse propagation along the path. This implies the knowledge of statistic characteristics of the propagation time fluctuations. Statement of the optimization problem seems to be premature under the conditions of insufficient information.

Moreover, at the first stage of the ACOUS Program the problem of experimental study of the propagation time fluctuation characteristics, i.e. practically "temperature" noises at the Arctic paths, is an independent and very important problem capable of determining the potential sensitivity of acoustic thermometry in the Arctic and defining the configuration of the future ACOUS network in this region. Thus, the papers [5] deal with the analysis of possible temporal sounding schemes, preceeding from the problem of determining tidal streams. The emission regimes suggested in them are aimed at maximum distinguishing of the "tidal" temperature signal, while one of the climatic measurement problems is maximum suppression (averaging) of similar noise signals for the thermometry of the signal climate. On the other hand, the duration and period of sounding sessions are related to the source resource and are important from the viewpoint of ecological aspects of the World ocean monitoring.

Under these conditions a compromise solution seems to be proper at the 1st stage of the ACOUS Program relalization.In this case at the beginning of the long-term experiment, emission will be rather often executed within 1 month, to get information on the parameters of propagation time fluctuations associated with the dynamic processes in the Arctic in a wide range of time scales (the background regime). Later, for example, beginning with the 2-nd month the sounding can be performed more rarely

according to the concept developed during the ATOC Program execution.

Therefore within a year operation period, the emission regimes can be determined in the following way:

a. Background operating regime - 1 month.

- duration of emission sessions τ = 20 - 30 min
- repetition rate of emission sessions T1 = 4 - 6 hours.

b. Main operating regime - 11 months

- duration of emission sessions τ = 20 - 30 min
- repetition rate of emission sessions T2 = 3 - 4 days

The number of sounding sessions within 1 year operation is presented in Table 1.

Table 1. Number of emission sessions within 1 year EC operation

T2,days \ T1,hours	4	6
3	290	230
4	260	200

The number of emission sessions at increased total duration of EC operation within 2 years (the background regime - 1 month) is given in Table 2.

Table 2. Number of emission sessions within 2 year EC operation

T1,hours / T2,days	4	6
3	410	350
4	350	290

The number of emitted pulses in an autonomous complex is limited by the energy capacity of the power supply source. However, the main limitation of the service life and even practical realizability of the complex is due to the necessity of isuring high efficiency of electroacoustic conversion of the emitting channel. The developed and long applied monopole resonance electromagnetic sources have rather high efficiency. The employed high-efficiency driving equipment permits to emit signals with different modulation types with relative frequency band of the order of 0.15 - 0.2. Such emitting systems have succesfully been used [6,7].

2.3. MAIN CHARACTERISTICS OF EMITTING COMPLEX

The above considerations enable us to formulate requirements to the main characteristics of emitting complex.

Table 3. Main characteristics of emitting complex

Resonant source frequency,Hz	20-30
Acoustic emission power,W	250
Relative frequency band of emission for 20 Hz for 30 Hz	 0.15 0.2
Emission type signal	MLS, CW
Duration of emission session,min	20-30
Number of emission sessions for 1 year operation for 2 year operation	 200/290 290/410
Long-term relative instability of time scale of complex	10^{-11}
Service period of complex,years	1 - 2
Submersion depth of source,m	100-150
Deployment depth of complex,m 1-st stage (1996-1997) 2-nd stage	 400-600 1000-2000

3. STRUCTURAL SCHEMES OF EMITTING COMPLEX

Let us consider two variants of the emitting complex: the autonomous and the cable one requiring the use of a coast station.

In the autonomous variant the power supply of the complex is provided by an autonomous electric supply source (cell battery). The EC operation is controlled by the built-in computer.

In the cable variant power supply of the complex and its control is performed through the main cable line from the coast station. The cable variant may include a cell battery operating in the constant recharge regime to insure pulse emission.

To solve the stated problems the emitting complex is to carry out the following functions and contain the appropriate functional subsystems:

- Electromagnetic type source with hydrostatic pressure compensation system.

- Source driving system enabling one to control power, frequency and phase of emitted signal.

- Frequency and time standart insuring the necessary time stability of emitted signal and synchronization of complex operation.

- System for determining current coordinates of the source by using bottom sonic underwater buoys .

- System for floating-up and elevating complex on surface with its search system.

- Main and additional electric power supply sources.

- System of emitted signal control responsible for measuring, processing and storage of each emitted signal parameters.

- System of complex control providing consistent operation of its consituent functional subsystems.

- System of external control and power supply needed for executing preliminary tests of the complex and for calibrating operations.

- Support equipment of underwater part comprising a hullmechanic part, cables, an anchor, etc.

- Support equipment of above-water part including spare tools and equipment.

The complex control system employing a computer insures its necessary functional flexibility and makes it a universal one. The data and instruction exchange between the computer and the rest functional parts of the complex is performed by appropriate interfaces. The operating regime of the complex is determined by the software set which can easily be changed depending on results of tests, calibration and experiment design. The external control regime is readily realized by exchanging software and data between the built-in computer and the operator controled external computer located either on the test vessel or at the coast and switched to the built-in computer through the external control connector and interface. The structural scheme of the autonomous emitting complex is shown in fig.11. In the cable variant of the emitting complex the structural scheme is mainly the same, though part of functional units can be arranged on the coast. The structural scheme of the cable variant is given in fig.12.

The emitting complex provides the possibility of testing immediately before its final deployment. These tests are aimed at determining otpimum parameters and operation modes practically at the place of deployment and at the designed submersion depth of EC. The tests are performed either from the supporting vessel or from surface of the ice station.

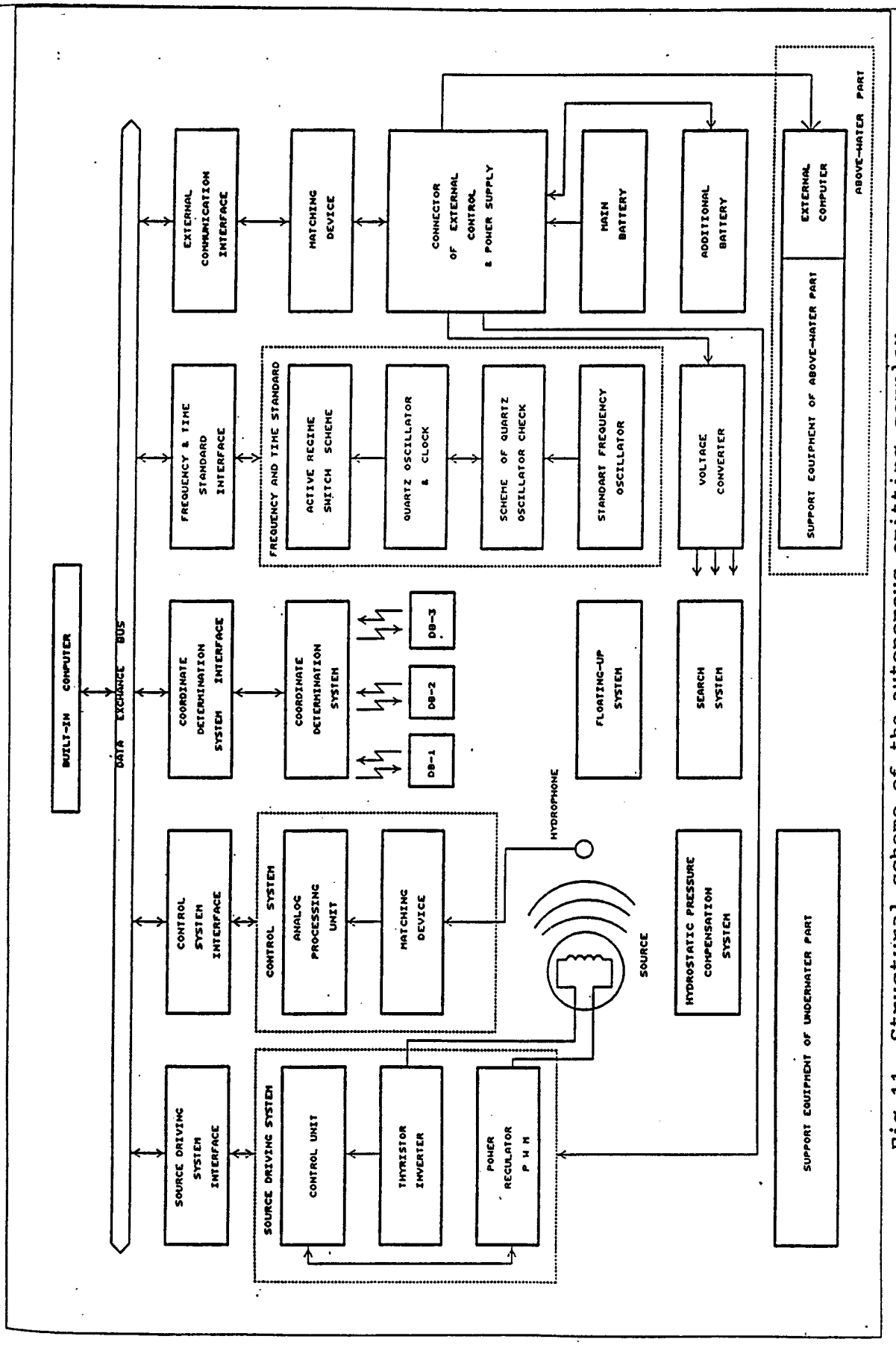

Fig.11. Structural scheme of the autonomous emitting complex

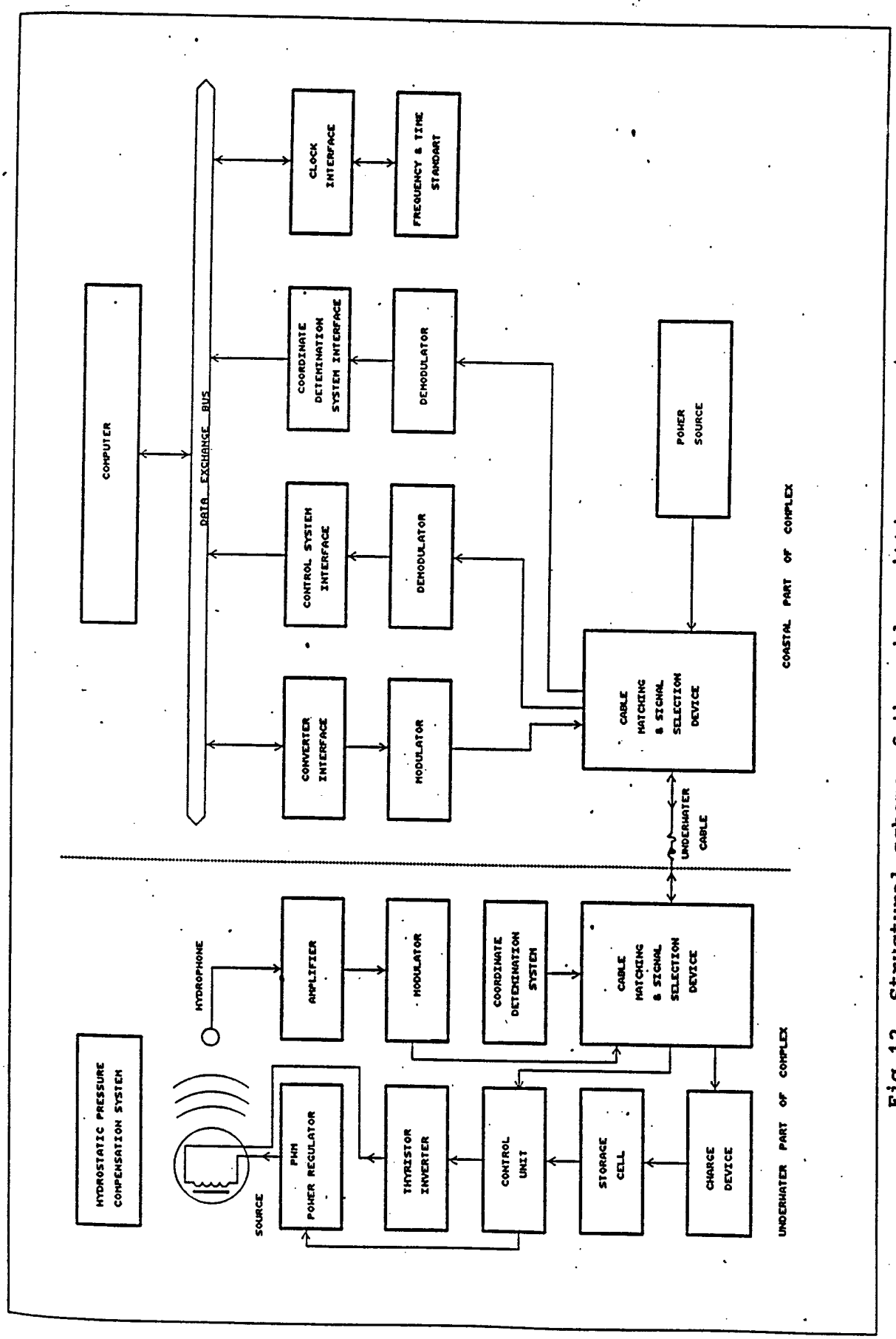

Fig.12. Structural scheme of the cable emitting complex

The emission mode, electric power supply, data exchange during the tests are controled by means of the cable through a special plug and the external control connector. The test results are used for the program correction of the control subprograms of the built-in computer, employing the external computer.

4. MAIN SUBSYSTEMS OF EMITTING COMPLEX

4.1 ELECTROMAGNETIC TYPE SOURCE

In a monopole source of a small wave size the emitted power is related to its volume variation as:

$$W = \frac{\rho\ \omega^4\ (dV)^2}{8\ \pi\ C} \qquad (4)$$

where ρ, C - are the water density and the sound speed in it, ω is the circular frequency, and dV is the amplitude of volume variation. For the 20 Hz frequency a power of 250 W is achieved at a volume variation of 6.15 dm^3, thus for the 30 Hz frequency we obtain 2.74 dm^3. Different design variants of electromagnetic sources are schematically shown in fig.13. The frequency bandwidth for a monopole is determined by its wave sizes and by the driving force margin in the electromagnetic system. It is known from experience that by using an electromagnet one can extend the emission band 2-3 times compared to the source band, the high efficiency being retained. If the attached water mass is much larger than the equivalent mass of the oscillating part of the emitting surface, the relative frequency band is yielded by the expression:

$$\Delta f/f = \frac{2\pi R}{\lambda} \qquad (5)$$

where R is the radius of the equivalent source sphere, λ is wave length . Employing the given values of the relative frequency band and taking into account that it can be extended three times by means of an electromagnet, we obtain from expression (5) that for 20 Hz R = 0.6 m, while for 30 Hz R = 0.53 m. If one knows the radius of the equivalent sphere, it is easy to calculate the emitting area and, hence, the source diameter. It follows from the calculations that the 20 Hz source is to have a diameter more than 2 m, while the 30 Hz source should be of a diameter 1.7 m. The consideration of technological problems from the viewpoint of the manufacturability and availability of appropriate equipment has shown that the source diameter should be less than two meters. Therefore, a diameter of 1.8 m is chosen to be the reference size for both frequencies.

Figure 14 deals with possible designs of the mechanical oscillation system of the source. The simplest oscillation system in the form of a single membrane (fig. 14-a) for the frequencies of our range is not suitable, since it has small emitting area. The most effective oscillation system is that with the emitting surface in the form of a piston and the elasticity in the form of two membranes (fig.14-c). This design combines the maximum emitting area, high oscillation stability at operating frequencies and small mechanical loads. However, the described design requires elastic decoupling of the piston and the case. It is technologically difficult to fabricate the decoupler from the material of the piston together with it, because this demands mechanical treatment of rather thin plates of large diameters. For these reasons we have chosen a compromise variant (fig.14-b) combining, to some certain extent, the simplicity of the first variant and the efficiency of the second one.

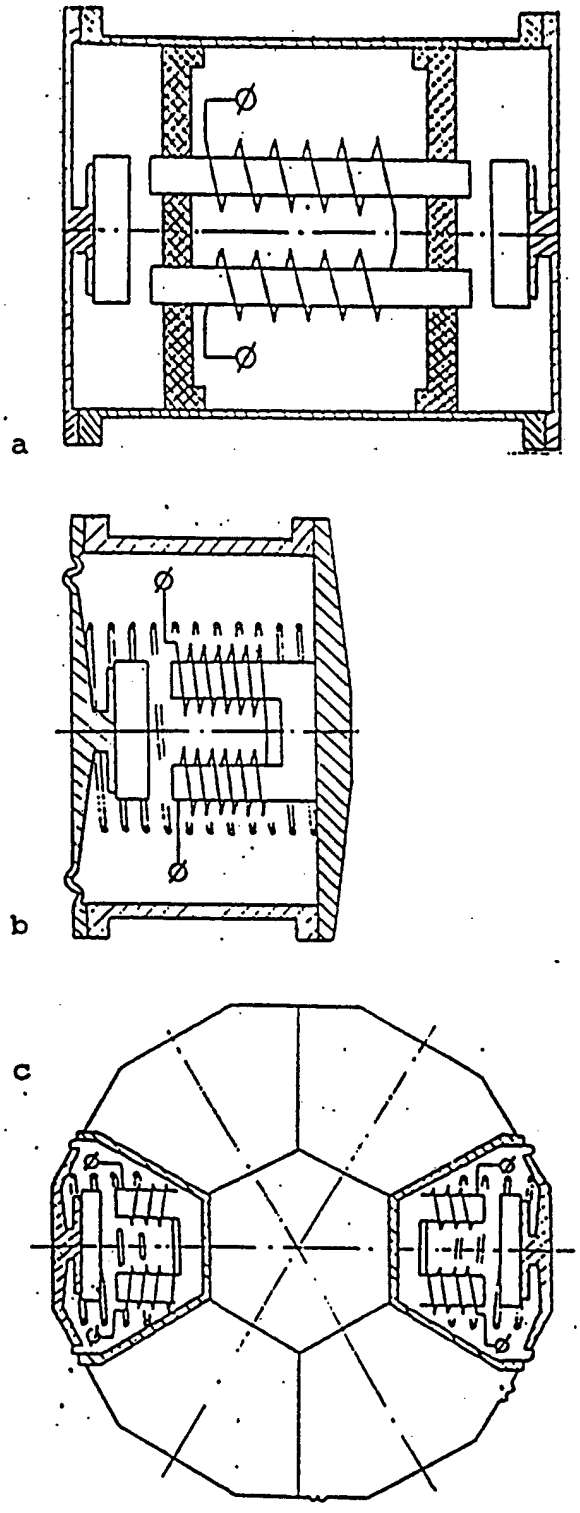

Fig.13. Electromagnetic type source designs.
a - plate design,
b - piston design,
c - design with several emitting surfaces.

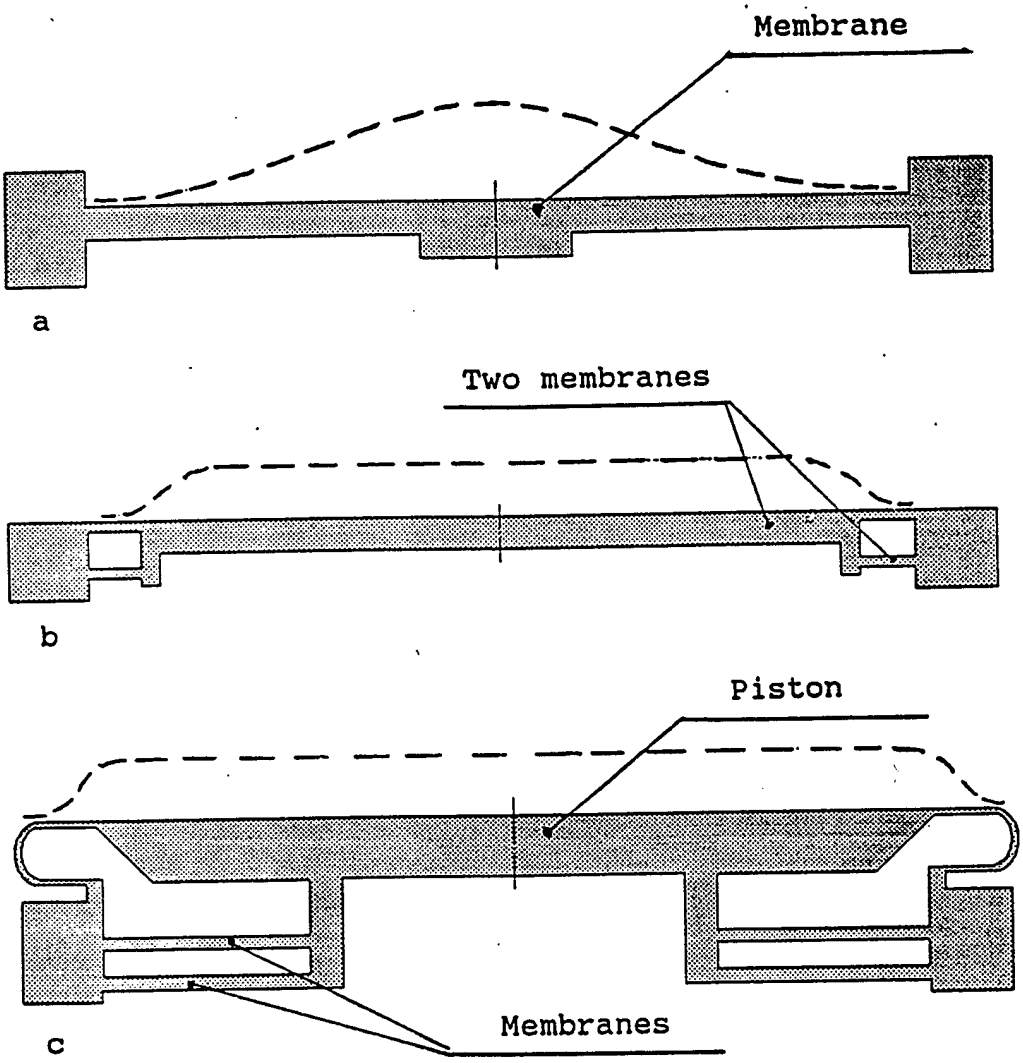

Fig.14. Mechanical oscillation system designs employed in source. (Dashed line shows the oscillation profile).
a - single-membrane design,
b - two-membrane design,
c - piston design.

The mechanical oscillation system was computed using an original program. The computation results are presented in the tables 4-7 given below. The meanings of the parameters (α,β,Δ) employed in optimization are explained in fig.15.

List of designations

Emitted power	W_e
Equivalent oscillating mass	M_e
Outer radius of operating membrane part	R
Inner radius of operating membrane part	a
Flange area	S_f
Increased thickness area in centre	S_c
Specific stiffness of flange	K_f
Elasticity modulus of material	E
Density of material	ρ
Membrane thickness at edge	h(R)
Membrane thickness at the centre	H
Emitting surface deflection caused by static pressure	W_{st}
Static mechanic loads per 1 atm.	σ_{st}
Equivalent emitting area	S_e
Stiffness coefficient of emitting surface	K
Relative emission band	$\Delta f/f$

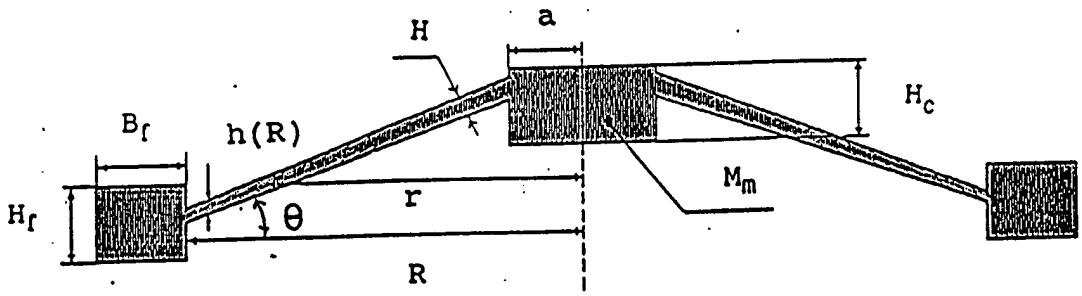

$\alpha = a/R \qquad \beta = H/h \qquad \Delta = \theta * R/a$

Fig.15. Hydroacoustic source membrane.

Table 4. α and β optimization, F = 20 Hz, material - steel.

Intput data:

W_e = 250 W		S_c	= 0.300E-02 m^2
R = 0.88 m		S_f	= 0.425E-02 m^2
M_e = 1120 kg		K_f	= 0.120E-03 m^4
ρ = 7800 kg/m^3		E	= 0.210E+12 N/m^2

α = 0.500 β = 1.5429 Δ = 0.0000

Normalized oscillation profile

1.000	0.996	0.980	0.954	0.918	0.873	0.821
0.762	0.697	0.628	0.556	0.482	0.407	0.333
0.262	0.195	0.134	0.082	0.040	0.012	0.000

Mechanic stress distribution (kg/mm^2)

8.67	8.07	7.32	6.64	5.87	5.17	4.47
3.75	3.02	2.28	1.52	0.73	0.10	0.10
1.47	2.85	3.87	4.95	6.13	7.35	8.67

F_{res} = 20.00 Hz	W_{st} =7.440 mm/1atm	σ_{st} =15.400 kg/mm^2
θ = 0.00	$\Delta f/f$ = 0.05	K = 1.921E+07 N/m
h(R) = 7.494 mm	S_e = 2.86 m^2	

Table 5. α and β optimization, F = 30 Hz, material - steel.

Intput data:

W_e = 250 W		S_c	= 0.300E-02 m^2
R = 0.88 m		S_f	= 0.425E-02 m^2
M_e = 1120 kg		K_f	= 0.120E-03 m^4
ρ = 7800 kg/m^3		E	= 0.210E+12 N/m^2

α = 0.500 β = 1.5638 Δ = 0.0000

Normalized oscillation profile

1.000	0.996	0.981	0.956	0.921	0.877	0.826
0.768	0.705	0.637	0.566	0.493	0.418	0.345
0.273	0.205	0.143	0.089	0.046	0.015	0.000

Mechanic stress distribution (kg/mm^2)

4.49	4.18	3.81	3.45	3.09	2.74	2.38
2.02	1.65	1.27	0.88	0.47	0.04	0.41
0.89	1.39	1.93	2.50	3.12	3.78	4.49

F_{res} = 30.00 Hz	W_{st} = 3.24 mm/1atm	σ_{st} = 8.373 kg/mm^2
θ = 0.00	$\Delta f/f$ = 0.079	K = 0.444E+08 N/m
h(R) = 9.928 mm	S_e = 2.89 m^2	

Table 6. β optimization, F = 20 Hz, material - aluminium.

Intput data: :

W_e = 250 W		S_c	= 0.300E-02 m^2
R = 0.88 m		S_f	= 0.425E-02 m^2
M_e = 960.0 kg		K_f	= 0.120E-03 m^4
ρ = 2700 kg/m^3		E	= 0.700E+11 kg/m^2

α = 0.500 β = 1.6116 Δ = 0.0000

Normalized oscillation profile

1.000	0.996	0.981	0.956	0.921	0.878	0.828
0.770	0.707	0.640	0.569	0.496	0.422	0.348
0.276	0.208	0.146	0.091	0.047	0.015	0.000

Mechanic stress distribution (kg/mm^2)

3.00	2.86	2.60	2.36	2.12	1.84	1.64
1.38	1.14	0.88	0.62	0.34	0.06	0.26
0.58	0.92	1.28	1.68	2.10	2.58	3.00

F_{res} = 20.00 Hz	W_{st} = 9.200 mm/1atm	σ_{st}=16.687 kg/mm^2
θ = 0.00	$\Delta f/f$ = 0.06	K = 1.590E+07 N/m
h(R) = 9.995 mm	S_e = 2.90 m^2	

Table 7. α and β optimization, F = 30 Hz, material - aluminium.

Intput data: :

W_e = 250 W		S_c	= 0.300E-02 m^2
R = 0.88 m		S_f	= 0.425E-02 m^2
M_e = 960.0 kg		K_f	= 0.120E-03 m^4
ρ = 2700 kg/m^3		E	= 0.700E+11 kg/m^2

α = 0.500 β = 1.6973 Δ = 0.0000

Normalized oscillation profile

1.000	0.997	0.983	0.959	0.927	0.887	0.839
0.785	0.725	0.660	0.591	0.520	0.447	0.374
0.301	0.232	0.167	0.108	0.059	0.022	0.000

Mechanic stress distribution (kg/mm^2)

1.80	1.63	1.49	1.34	1.24	1.12	0.99
0.85	0.72	0.58	0.44	0.29	0.13	0.05
0.23	0.43	0.69	0.88	1.14	1.42	1.80

F_{res} = 30.00 Hz	W_{st} = 4.00 mm/1atm	σ_{st}= 9.517 kg/mm^2
θ = 0.00	$\Delta f/f$ = 0.09	K = 0.370E+08 N/m
h(R) = 13.036 mm	S_e = 2.95 m^2	

The optimized class of membrane shapes is shown in fig.15. Only plane membranes $\Delta = 0$ were considered for the sake of techological simplicity. At 20 Hz and a power of 250 W the membrane motion is 2.5 mm, while for 30 Hz it equals 1 mm. To provide high electromechanic efficiency the gap in the electromagnet should be the least possible. For the 20 Hz source the 4 mm gap can be chosen, while for 30 Hz 3 mm. The shape and sizes of the magnetic circuit are designed for the efficiencies of 85% and 92%, respectively, the rated current of the winding 3 A, and the winding voltage 700 V. The voltage and current consumed from the power source amount, respectively, to 240 V and 2 A. In the 30 Hz source only the thicknesses of the operating membrane parts and the source height are varied.

If the equivalent elasticity of the mechanical oscillation system and the volume of the internal source cavity are known, one can find out the variation of the resonance frequency in the source versus depth using the expression:

$$df/dh = \frac{æ\, S_e^2\, 10^5}{2\, k\, V} \qquad (6)$$

where V is the volume of the source air cavity, p is the pressure, S_e is the equivalent emission area, æ is the adiabatic coefficient, k is the elasticity coefficient of the oscillation system (according to the computations). For steel source for F = 20 Hz and V = 2 m^3 we obtain df/dh = 0.03 Hz/m. An analogical frequency variation for 30 Hz is obtained at V = 0.85 m^3.

The design static deflections of the mechanical oscillation system of this source W_{st} for the difference pressure outside and inside the source equal to 1 atmosphere are, respectively, 7.4 mm and 3.2 mm. In the operative source the variation of gaps in the magnetic system is to be at least two times less than the

operating motion. This yields the necessary accuracy of the hydrostatic pressure compensation equal, respectively, to 0.15 atm. and 0.2 atm. Below is the table of design parameters for the 20 Hz and 30 Hz sources:

Table 8. Design parameters for 20 Hz source

material	steel	aluminium
diameter (m)	1.8	1.8
height (m)	0.9	0.9
mass (kg)	2000	1000
volume (m^3)	2.3	2.3
relative width of operating frequencies (%)	15	17
emission power (W)	250	250
mechanic stress in oscillation system (kg/mm^2)	8.67	3.0
electromechanic efficiency at resonance frequency (%)	85	82
mechanoacoustic efficiency (%)	80	70
volume of internal air cavity (m^3)	2.0	2.0
resonance frequency gradient in depth (Hz/m)	0.029	0.031
pressure difference resistance (atm.)	0.95	0.9
rated winding voltage (V)	700	700
rated current (A)	3.0	3.0
equivalent emission area (m^2)	2.9	2.9
rated operating motion (mm)	2.0	2.0
pressure compensation accuracy	0.15	0.13
source resource (of oscillation cycles)	10^9	10^9

Table 9. Design parameters for 30 Hz source

material	steel	aluminium
diameter (m)	1.8	1.8
height (m)	0.4	0.4
mass (kg)	1500	750
volume (m^3)	1	1
relative width of operating frequencies (%)	20	25
emission power (W)	250	250
mechanic stress in oscillation system (kg/mm^2)	3.49	1.8
electromechanic efficiency at resonance frequency (%)	92	90
mechanoacoustic efficiency (%)	80	75
volume of internal air cavity (m^3)	0.8	0.8
resonance frequency gradient in depth (Hz/m)	0.025	0.027
pressure difference resistance (atm.)	1.72	1.6
rated winding voltage (V)	400	400
rated current (A)	3.0	3.0
equivalent emission area (m^2)	2.9	2.9
rated operating motion (mm)	1.0	1.0
pressure compensation accuracy	0.25	0.22
source resource (of oscillation cycles)	10^9	10^9

High mechanoacoustic efficiency can be obtained only if one maximally reduces the friction loss mainly occurred at joints of bending membranes. This problem can radically be solved by means of welding. In this case the internal and external flanges of the mechanical oscillation system become monolith, while in the single bolt joint the strain is slight and thus the friction loss is also small. Welding has not been earlier applied in manufacturing mechanic oscillation systems of sources, since high-strength alloys of low weldability were used to fabricate an oscillation system. In the suggested design the mechanic loss is reduced 3-4 times and it would be logical to employ high-technology and frequent steel qualities. To estimate their applicability the following alloy samples have been tested: steel 3, the AK 25 hull plate, the AMG 61 hull aluminium alloy, the 3V titanium alloy. All the materials have good weldability. To determine the strength of welds, samples with welds were tested in the dangerous area. The test basis is 10^8 oscillation cycles. As the samples were cyclically loaded, their resonance frequency were continuously controlled, which furnished information on the elasticity modulus stability. The fatigue curves experimentally obtained for the tested samples are presented in figs.16 and 17. Figure 18 displays typical curves of the resonance frequency versus the number of oscillation cycles. The conclusion can be drawn from the tests that at design loads these materials provide at least a triple required reliability in strength. The stability of the elastic properties of materials at cyclic loads in the necessary range of mechanic stresses is rahter high. Proceeding from the said above, the source design implied the most abundant material - steel 3.

4.2 SOURCE DRIVING SYSTEM

To drive electromagnetic sources we have long and successfully applied electron schemes of the class of resonance thyristor inverters. The advantage of such schemes is their perfect matching to the inductive input impedance of the source.

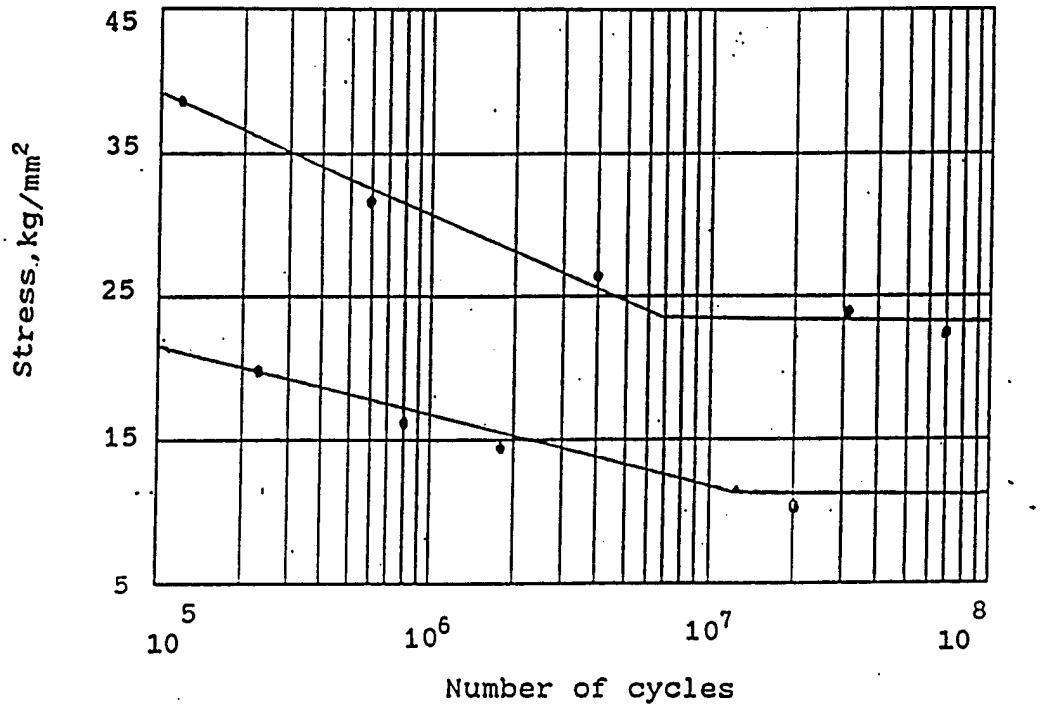

Fig.16. Fatigue curves for AMG6 aluminium alloy (lower curve) and steel 3 (upper curve).

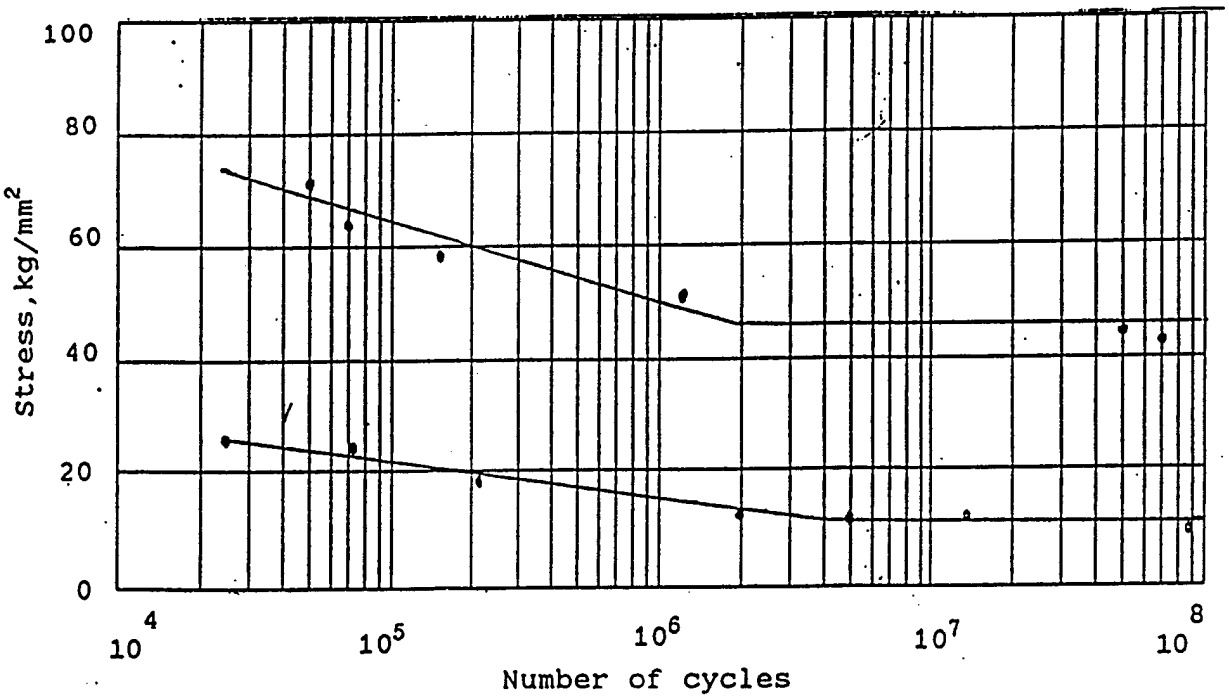

Fig.17. Fatigue curves for AK25 steel (upper curve) and steel 3 welded seam (lower curve).

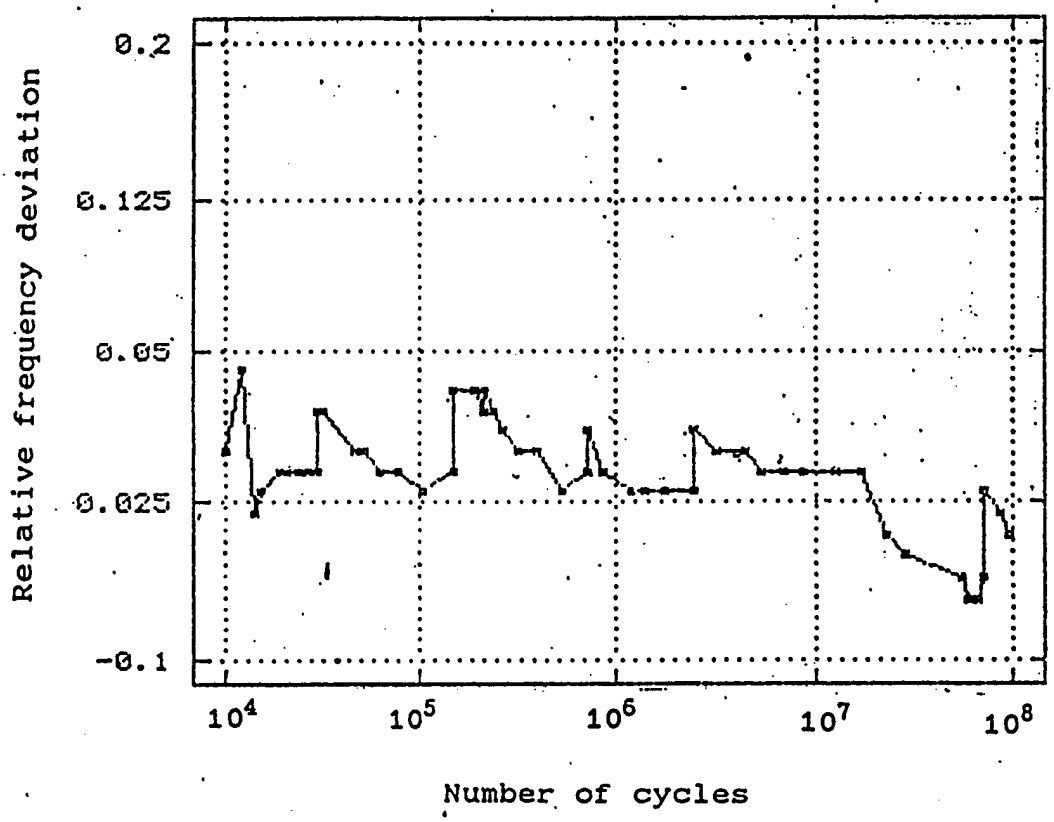

Fig.18. Frequency deviation of natural oscillations versus number of oscillation cycles for sample of steel 3.

Being key devices, the resonance thyristor inverters have very high conversion efficiency achieving 95%. The produced thyristors can commutate electric signals of high current and voltage and withstand multiple loads, thus the reliability of such devices is rather high.

Figure 19 exhibits a scheme of the bridge resonance thyristor inverter together with the emission power control scheme. Epures of voltages and currents for the steady-state oscillation regime are shown in fig.20.

The scheme operates as follows. When the capacitor C is not recharged through the inductance L of the source winding, all electron keys are closed, current does not run, the condenser C stores the accumulated charge and its voltage is practically constant. Rectangular pulses of the duration T_a and the repetition rate T reach the control scheme input. When the leading front of the pulse arrives, the controlled V6 key is opened as well as a pair of uncontrolled keys in the thyristor bridge diagonal, for example, V3 and V2. The capacitor C is recharged through the power source and the winding. Current running through the winding creates the force exciting oscillations in the mechanic oscillation system of the source. In time T_a the V6 key is closed and current starts to run through the V2 power diode. It is evident that by varying the time T_a we either increase or decrease the energy part transmitted from the power source to the circuit and can thereby control the radiation power. When current in the circuit practically vanishes, the V3 and V2 uncontrolled keys will close themselves and the system will reset the initial state, only the charge of the capacitor C being changed for the opposite one. This state will be retained up to the next pulse arrival, after that the process will repeat with the open V1 and V4 keys. The capacitor recharge time T_r is determined by the resonance frequency of the LC circuit. The capacitor C should be chosen so that T_r be less than T.

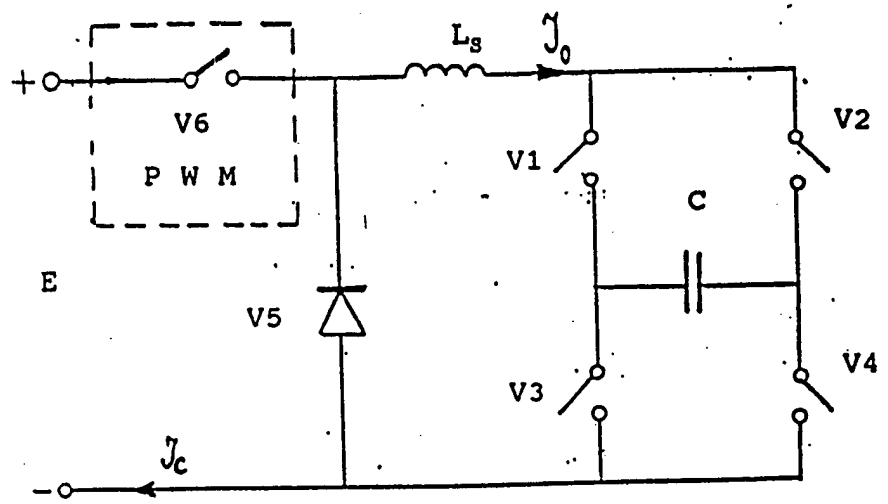

Fig.19. Scheme of emission driving device

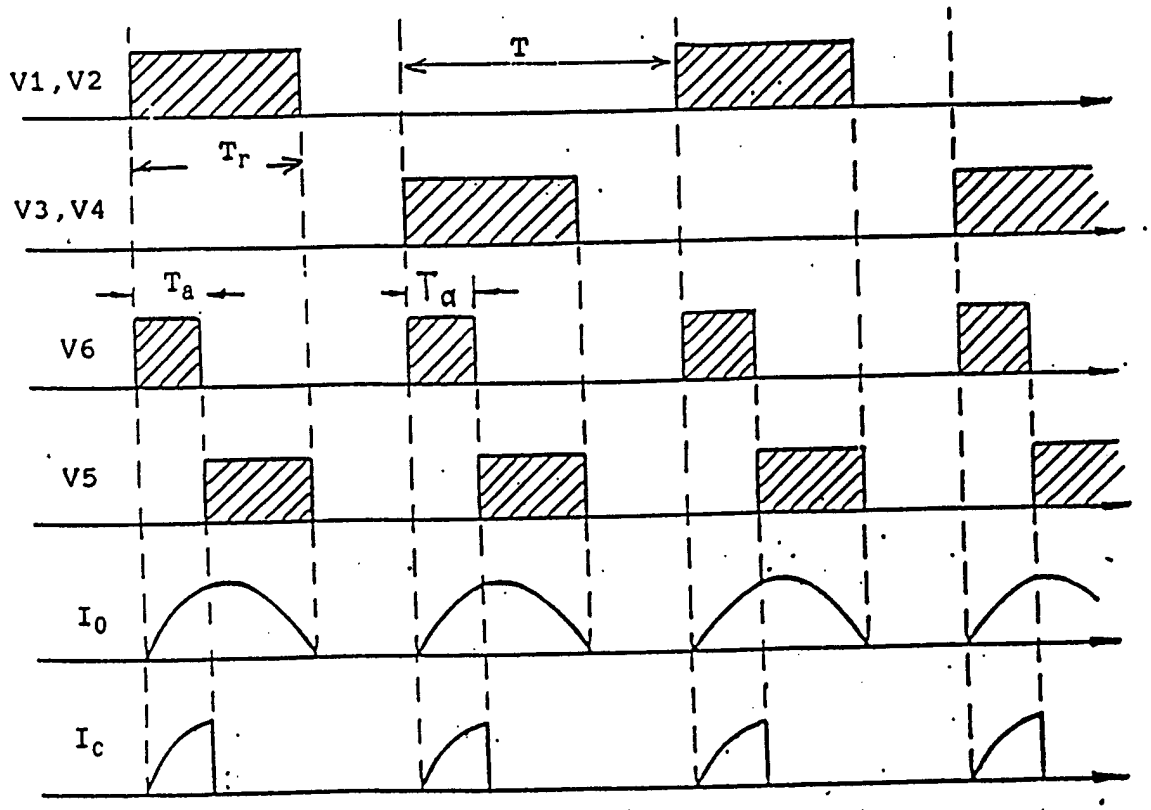

Fig.20. Epures of currents and voltages in the emission driving device.

The principle of the nonlinear excitation of the source is realized in the simple scheme described above. A specific feature of the scheme is the dependence between the driving frequency of mechanic oscillations and the pulse repetition rate T, while the electric processes in the circuit correspond to the sequential resonance and are determined by the time T_r irrespective of the period value T. Thus, perfect matching of the electric and mechanic parts is achieved in a rather wide frequency band. Another useful feature of this scheme is its "tendency" to maintaining constant emission power at a varying emission frequency if a high-efficiency source is connected to it.

Figure 21 deals with experimentally obtained frequency dependences of the emission level on the frequency of the source prototype of the frequency 65 Hz. Curve 1 is obtained at constant amplitude current in the source winding or at a constant value of the driving force and corresponds to the frequency characteristic of the oscillation system of the source. Curve 2 is obtained for the source operating with an inverter. By comparing them we see how effective is the frequency band extension in the second case. The observed effect can be explained rather easily. If the conversion efficiency is high, the main component of the resistance loss of the circuit R is the resistance of the source emission converted to the electric part. In the case of the frequency mismatch from the resonance the electromagnetic coupling coefficient of the source decreases and consequently the loss resistance of the source also diminishes. The Q-factor of the circuit increases and since the processes in it always correspond to the exact series resonance, the winding current increases and compensates the emission power decrease.

Practically none high-power conversion device can reliably operate if only functionally needed units are provided, particularly for the reactive or resonance character of the load as in our case. Only the use of protection schemes permits to

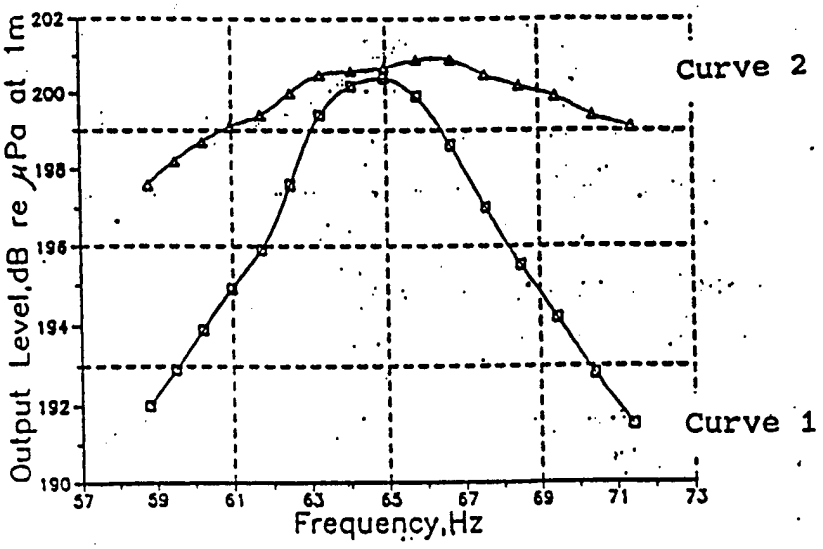

Fig.21. Amplitude-frequency characteristics of the source prototype. (Curve 1 for constant amplitude of source winding current I, curve 2 for source operating with an inverter).

solve the problem of the service reliability of the driving system. Under the conditions of an unattended complex one can employ protection facilities against malfunctions of the reversible character. Analysis of the redundancy capability of the power part of the driving system has demonstrated that additional high-power switchers should be furnished in this case, the reliability provision of which eliminates the redundancy benefits. Therefore, the main method of the reliability provision is the choice of power elements of the scheme with large margin of admissible parameters and high reliability indices. The realization of the thyristor bridge in home-produced thyristors is not difficult. The situation with the V2 diode and other power elements except for the V1 electron key is analogous. It is more preferrable to use high-power foreign-produced IGFET or combined transistors. They have much less control loss than bipolar transistors.

Sometimes thyristors can open spontaneously. This happens randomly and seldom, but if it does and, for example, the V3 and V5 keys open simultaneously, the scheme will change over to the uncontrolled regime of the short circuit. This phenomenon is called the reversal of the inverter. The reversal can also occur if pulses of unsuitable frequency or phase are supplied to the inverter input as a result of malfunation in the pulse formation system, for example, in the computer. To eliminate the emergency situation of this kind, a protection scheme is forseen consisting of a rapid logical device that determines the reversal instant and disconnects the power source thereby closing the V1 key. Information on emergency is transmitted to the built-in computer. Further action can be different depending on the program solutions. Blocking can be removed in short time needed to restore normal operation of the scheme, part of the signal being lost. The emission regime can be repeated, etc.

Another cause of emergency can be abrupt change of frequency and master pulse duration occurred as a result of malfunction in

pulse formation systems. Current and voltage in the circuit can break power elements of the scheme and the source electromagnet. To eliminate such regimes a non-disconnecting protection scheme is provided which analyses the input pulse parameters, the current and voltage in the power circuit and, if necessary, corrects input pulses preventing the excess of the limiting values of the parameters. Information on the protection scheme operation is to be transmitted to the built-ine computer, where it can be used to determine errors or to make hardcopying. The suggested protection facilities permit to provide high reliability of the driving system.

In the active regime the emission control systems consume a power of 5 W, in the waiting regime the power consumption is negligibly small.

4.3 FREQUENCY AND TIME STANDARD

The required long-term time stability of emission could be provided by applying atomic frequency standard. However, even a small atomic clock consumes a power of 16 W, which is inadmissible for continuous work during a year. For this reason we employ lower energy consumption methods to insure the necessary stability. The portable quartz oscillator SULZER MODEL 1115 CRYSTAL OSCILLATOR possesses stability of 10^{-9} within 24 hours and consumes a power of 0.3 W for the power supply voltage of 12-15 V. The output signal frequency is 5 MHz. This oscillator can provide the necessary stability during approximately 5 days. To keep the required accuracy of time reading during a year and to calculate time errors, one can employ a rubidium frequency standard - the TCH1-84 OSCILLATOR with a relative error of the frequency restoration from switch to switch 10^{-10} - 10^{-11}. If the procedure of the error determination by the quartz oscillator is performed once a day, the needed accuracy can be provided. The TCH1-84 OSCILLATOR consumes a power of 70 W within 5 minute operation and 16 W in

the operating regime. The output frequency of the oscillator signal is 10^7 Hz. The functional diagram of the frequency and time standard is shown in fig.22. A pulse meter records the number of pulses of the output frequency of the rubidium oscillator between the time marks produced by the clock with a quartz oscillator. The required accuracy is insured by correcting the quartz clock by means of measuring the clock interval of the time of pulse formed by the rubidium standard. The average power consumed by the correction system amounts to 1 W, while the average power of the whole frequency and time system does not exceed 2 W. To obtain the necessary power supply voltages, one can employ the POWER MODULE 5124 CONVERTER.

4.4 BUILT-IN COMPUTER

A computer of the type "Micro PC" - 6012 PC Control card is adapted to operate in complicated service conditions. This is a compatible computer with the operating temperature range from - 40 to + 85 degrees Centigrade having the sizes of 114x124x20 mm and low power consumption of the order of 3 W. Average time of no-failure operation equal to 100000 hours guarantees high reliability. The computer is made by the OCTAGON SYSTEMS company (USA) according to the ISO 90001 quality standard. Computers are employed in the control-measuring equipment of the Space Shuttle. The computer may include the set of standard cards, such as:

(A) Control card - 6012 PC.
(B) 4 Mb solid-state disc - 5805.
(C) Isolated digital I/O - 5624.
(D) Power module - 5124.

The computer can be inoperative for a long time. It is switched on by a special program device (see fig.22). The time of the next switch is assigned by the computer itself in the previous session of the active regime. The computation power of

the computer multiply exceeds the requirements of the emitting complex and its architecture permits to rather easily realize the necessary functions of the complex.

4.5 EMISSION CONTROL SYSTEM

The emission control system is designed for maintaining the required parameters of the emitted signal, for measuring and analysing the parameters of each radiated pulse within the entire operation period and for hardcopying the necessary set of the emitted signal parameters. The functional scheme of the control system is shown in fig.23. A standard piezoceramic hydrophone can be used as a receiver. The hydrophone has high stability of the sensitivity and the submersion depth exceeding the needed one. To obtain a spherically isotropic acoustic signal, the hydrophone should be placed at a distance equal to double maximum geometric sizes of the complex, i.e. at approximately 5 meters. The protection device prevents any possible failure of the hydrophone electron system, caused by the action of static electricity or signals produced by shocks or sharp pressure overfall. The band-pass filter with a matching device forms a sufficient band for further analog-digital conversion of the measured signal. Further correlation processing of the complex signal can be performed using a computer copy and the correlation function parameters can be stored. This needs the memory of the order of 1 Kb. All electronics can be made on the board in the frame of the built-in computer and be fed by its power module. Power supply of the hydrophone is provided by the current source preventing short circuit at the power module output in the case of flow in the hydrophone or a cable. The consumed power of the control system is 0.05 W. Due to small time of the built-in computer operating the average consumed power in active mode is negligibly small.

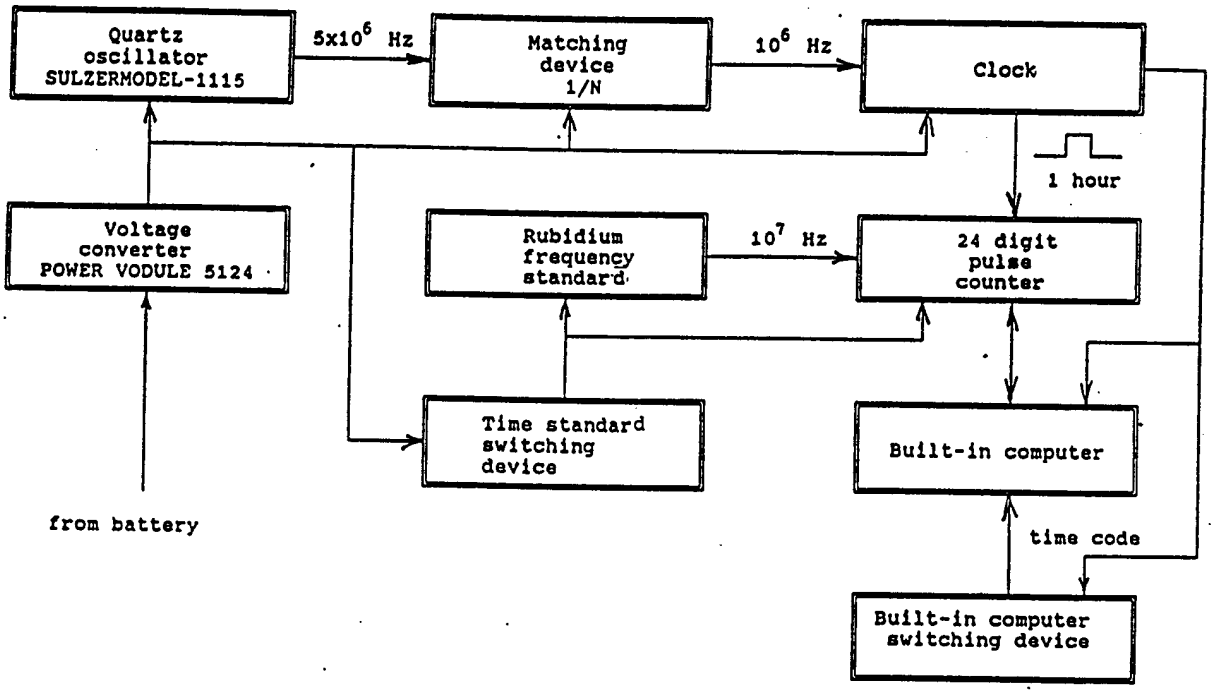

Fig. 22. Block diagram of frequency and time standard

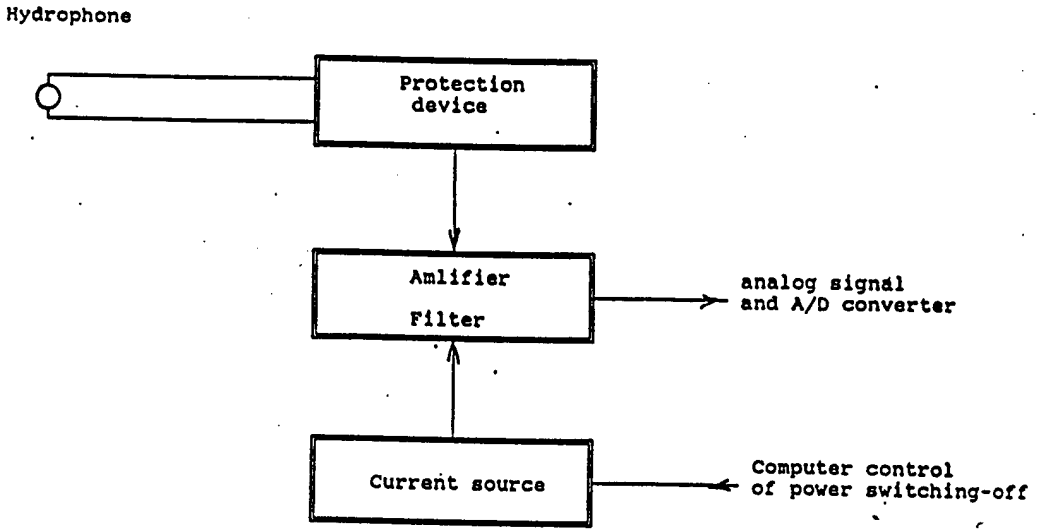

Fig. 23. Block diagram of control scheme

4.6 COORDINATE DETERMINATION SYSTEM

The importance of the coordinate determination system especially for the moored variant is comparable with that of the frequency and time system. The necessary accuracy of determining the current dispacement of location from some average value is of the order of several meters.

A similar system is used in the AVATAR system. It consists of a hydroacoustic receiving transmitter placed on the hullmechanic part of the complex and three bottom buoy - transponders. The distance between the buoy and the complex anchor should be of the order of several kilometers. To provide the required accuracy of coordinate measurements, the measurement accuracy of the time interval between the request signal emission and the response signals must not be worse than 0.5 ms, for which the carrying frequency of the system is to be of the order of 10 kHz.

4.7 ELECTRIC POWER SUPPLY SOURCES

4.7.1. Electric power supply source for autonomous emitting complex

Main specifications of the power supply source:

- rated voltage (V)	240
- discharge pulse duration (s)	1200 - 1800
- discharge current (A)	2.0
- internal resistance not more than (Ohm)	0.5
- environmental temperature (C.)	2.0-4.0
- pressure inside container (Pa)	10^5

A comparative analysis of the chemical current sources was performed for storage cells and batteries. The 12ER 20S-30 lithium batteries of capacity 300 amphere-hour and voltage 41 V are most suitable according to the specific and economic

indices. These batteries produced in hermetic vibro-shockproof case with 100 V electric insulation are designed for the aircraft industry. The battery is minimized according to its weight-size indices. The probability of no-failure operation of the battery is not less than 0.996. The maximum service time is 650 days.

The power source must comprise six batteries connected in series. The source mass is 300 kg, its volume is 0.35 m^3. For the pulse duration of 20 min the energy content is sufficient for 500 pulses, for the duration of 30 min - 300 pulses.

In accordance with Tables 1 and 2 (section 2.2) this power source will provide the necessary number of emission sessions for the complex operation during the period from 1 to 2 years for various combinations of the emission parameters in the background and main operating regimes (τ = 20-30 min, T1 = 4-6 hours, T2 = 3 - 4 days).

4.7.2. Additional electric power supply source for autonomous emitting complex

The additional source is to provide operation of all devices except for the thyristor inverter. The energy consumed by the devices within a year amounts to:

	kilowatt-hour
- rubidium frequency and time standard	8.0
- quartz oscillator	3.0
- thyristor inverter control	0.5
- built-in computer	2.0
- other	0.5
Total, energy	13.0

Can be used in the source the 9ER 20S-16 lithium batteries of voltage 30 V and capacity 150 A.hour. The source voltage directly matches the converter - Power module - 5124. The source should have 3 batteries. The batteries are connected parallel with diode decouplers. The total source weight is 75 kg, the volume is 36 dm^3.

4.7.3. Power supply source for cable emitting complex

The accumulator supply source of capacity sufficient for emitting a single pulse is most suitable in this case. If even six pulses are emitted a day, the duty cycle equals 8 - 12 and, thus, the storage battery can be recharged by small current, not to impose any restrictions on the length and type of the sea cable. In the source one can employ the nickel-cadmium hermetic inattainable cell of the NKGK-11 D type of capacity 11 A-hours and voltage 1.36 V. The discharge energy for a single pulse amounts to 10% of the cell capacity and enables the cell to withstand more than 1000 charge cycles. The guarantee service period of the cell is 10 years. The source is to contain 175 cells connected in series. The total weight of the power supply source is 100 kg, its volume is 40 dm^3. To provide high reliability the cells can be grouped, for example, in fives and a diode can be connected parallel to each group. In this case if a contact is failed in any cell the voltage of the entire power supply source will decrease only by 6 V.

5. WEIGHT-SIZE AND ENERGY CHARACTERISTICS OF EMITTING COMPLEX.

The weight-size and energy characteristics of EC are, primarily, dependent on the corresponding characteristics of the source. We shall estimate them using a steel 3 source with a resonance frequency of 20 Hz. This choice is due to availability of this material and higher technology applied to fabricate such

a source. Specification of the source are presented in table 10.

Table 10. Source specification

Name	Value
Emission frequency,Hz	20
Diameter,m	1.8
Height,m	0.9
Outer volume,m^3	2.25
Inner volume,m^3	2.0
Mass,t	2.0

Table 11 deals with weights and volumes of the moored autonomous EC subsystems with emission frequency - 20 Hz.

Table 11. Main EC subsystems weights and volumes.

Name	P,t	V, m^3
Source	2.0	2.25
Electric power supply battery	0.35	-
Container for battery	0.27	0.94
Other equipment	0.5	0.35
Container for other equipment	0.54	1.88
Automomous outboard equipment	0.3	0.15
Pressure compensation system	0.12	0.4
Frame	0.5	0.06
Buoyancy units	0.05	0.1
Total	4.63	6.13
Positive EC buoyancy	1.5	

As is shown in section 4.7.1, this autonomous complex provide 500 emission sessions for the 20-minute emission duration and and 300 emission sessions for the 30-minute duration, respectively.

This guarantees the EC operation during at least one-two years, the 1-year operation being provided at any variations of emission parameters. At the same time it should be noted that the number of cycles for the complex operating during 2 years in the worst mode is 1.5×10^7 cycles. This value is more than an order smaller than the source resource which is close to a value of 10^9 cycles.

It seems to be interesting in this connection to estimate the possibilities of applying a source with the characteristics necessary for high-quality emission of signals at a shorter path of about 900 km, at the first stage of the ACOUS Program.

As is shown in section 2.1, the following source parameters are to be provided:

- frequency (Hz)	-	20	30
- emission power (W)	-	2.5	25

The analysis of the source design has shown that it is not proper to sharply reduce its sizes. At small sizes it is impossible to obtain the high efficiency equal in this case to several percents. Thus, the size and cost of the electric power supply source will slightly decrease. There will simultaneously grow the complexity of hydrostatic pressure compensation and of the insurance of reliability of the source. The high efficiency and reliability of the source can simultaneously be provided only if its equivalent wave size is retained. However, at small powers the oscillation amplitude of the emitting surface decreases abruptly, as well as cyclic mechanic loads. In this case the emitting surface can be optimized not for the minimum

mechanic loads on assigned emitting area but, vice versa, for the maximum emitting area, and hence, for the maximum wave size of the source at assigned mechanic loads. The performed calculations have demonstrated that if all acoustic parameters of sources except for power are conserved, the following parameters can be obtained:

material	steel	steel	aluminium	aluminium
frequency, Hz	20	30	20	30
diameter, m	1.6	1.4	1.6	1.4
height, m	0.9	0.4	0.9	0.4
mass, kg	1100	500	600	300
displacement,kg	1800	615	1800	615

By conserving the high efficiency of the source, we can reduce at least several times the electric capacity of the battery, and thus, its size and weight, and increase the source operation time by 3 - 5 years. It should be noted that this variations of the source characteristics may essentially change the entire source design. But this requires thorough consideration of the problems.

6. INSTALLATION AND ELEVATION OF EMITTING COMPLEX

The moored autonomous EC variant is submerged to the serviceable position from board the ship as follows (fig.24) - first the bulk anchor is carried overboard and submerged using the total length of the cable, then the source is carried overboard and submerged to the operating depth (up to contact of the anchor and soil) by means of an auxiliary cable. After EC is deployed in the serviceable position the auxiliary cable is lifted on board the ship. EC is elevated to the surface by disconnecting EC from the anchor cable using an acoustic disconnector (fig.25), after which EC floats up to the surface

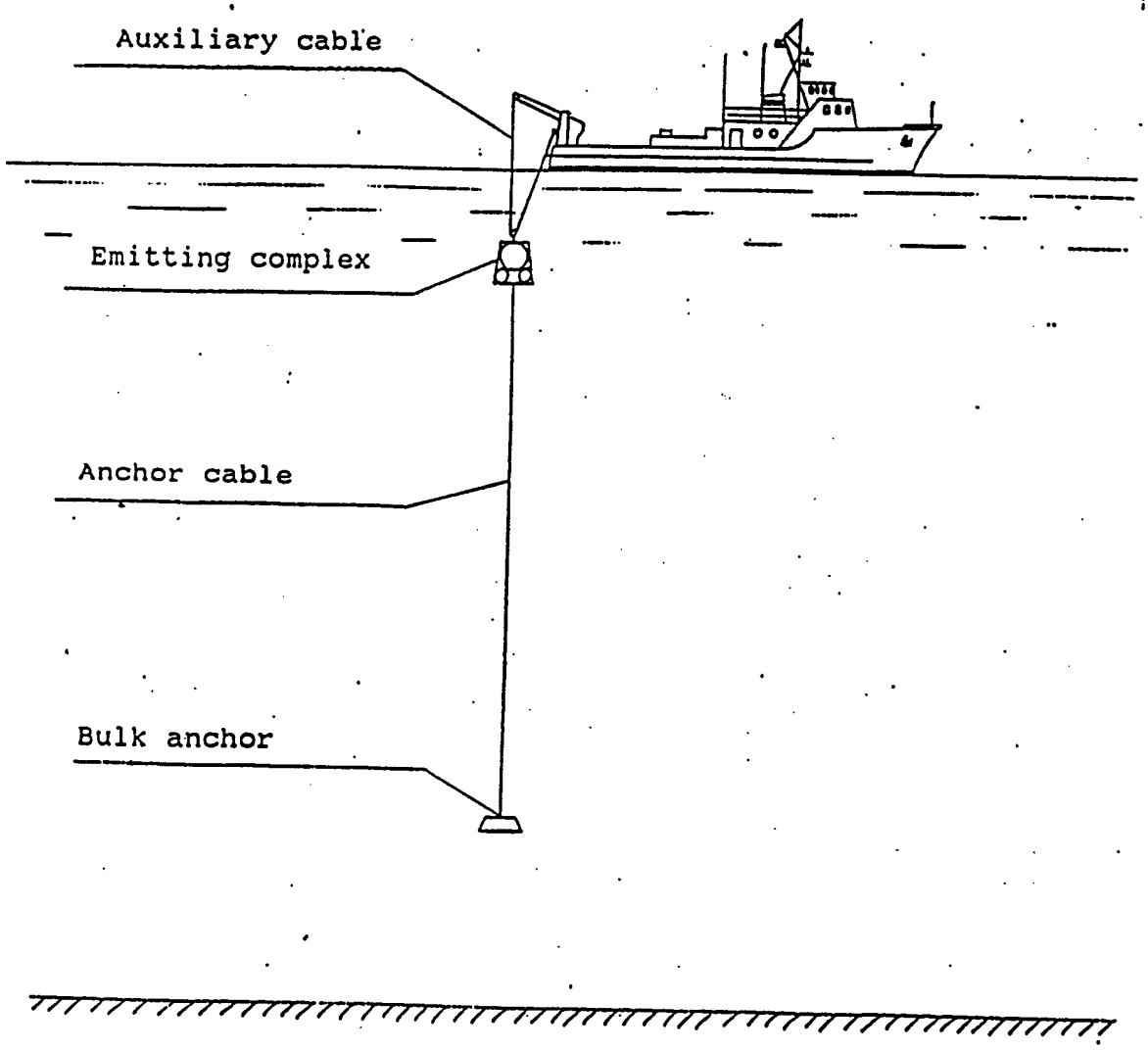

Fig.24. Installation of autonomous emitting complex in serviceable condition. Complex is submerged by means of cable to operating depth, until anchor and soil contact.

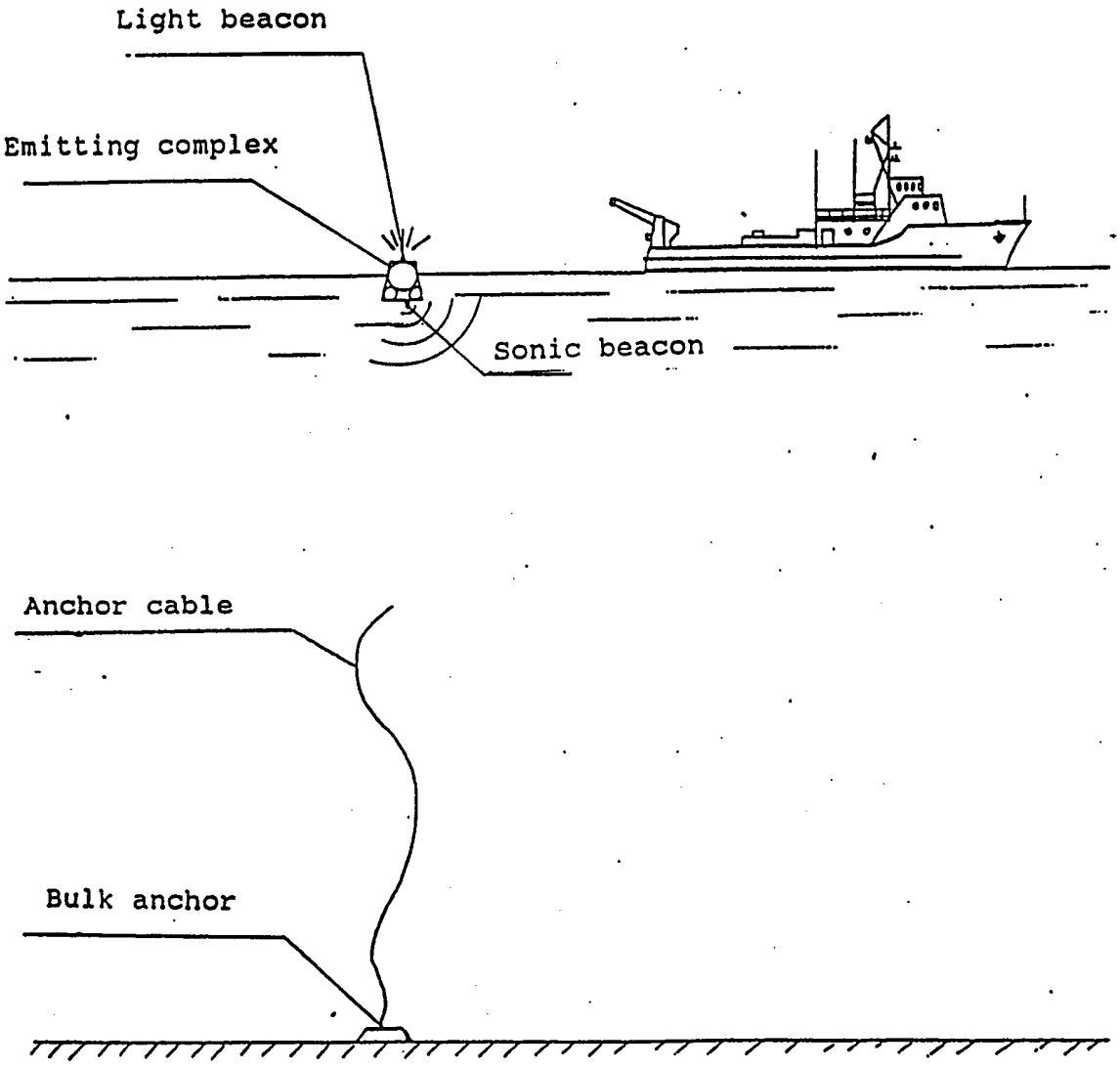

Fig.25. Elevation of autonomous emitting complex on surface. After disconnection of anchor cable using acoustic disconnector, complex floats up on surface due to its positive buoyancy. Anchor cable is submerged to bottom. Complex is detected using light and sonic beacons.

under the action of its positive buoyancy (1.5 t). EC is detected by means of the light and sonic beacons and a radar reflector mounted on it.

To unload the source from the external hydrostatic pressure, a simple and rather reliable pressure compensation system (PCS) is uitilized. When EC is being submerged to the serviceable position, a hose is released from board the ship, using which compressed air is constantly supplied to the source through the nonreturn valve. The air excess is constantly released from the source through the safety valve providing the pressure excess in the internal cavity of the source compared to the external hydrostatic pressure of about 0.2 atm. After EC deployment the air supply ceases and the hose is disconnected from EC. PCS can be supplemented with a soft pressure compensator to compensate the EC oversumbersion caused by underwater currents during the operation period. When the source is elevated the excess pressure is released through the special air release valve.

The carried out hydrodynamic calculations of the moored EC variant have demonstrated that for the positive buoyancy of about 1.5 t, the oversubmersion of EC caused by underwater currents will not be larger than several centimetres, and the horizontal displacement lies within the limits 3.7 - 0.6 m for the anchor cable length of 350 m and maximum speeds of currents at the EC submersion depths 0.25-0.1 m/s, respectively. A steel cable of diameter 12.5 with the breaking load of about 6 t or a kapron rope of analogous strength can be used as an anchor cable. The weight of the steel anchor cable in water is about 0.1 t. To keep EC at the assigned point of the area, the gravitational type anchor of mass about 2 t is needed.

To deploy EC in the serviceable position, auxiliary fleet vessels of the following types can be employed: the MB 148 tug, a cable ship, small and large special ships (killectors) . All of them have appropriate freight host facilities (catcranes,

cargo booms, winches, etc.) of displacement not less than 6 t.

A similar deployment scheme can also be used for the deployment from surface of the ice station. In this case some spread in the EC submersion values may occur because of ice drift but this circumstance is not to bring about essential problems in installation and service of the complex.

7. COST ESTIMATE OF AUTONOMOUS EMITTING COMPLEX DEVELOPMENT AND INSTALLATION

At the first stage of the ACOUS Program (1996-1997) we recommend to use the autonomous emitting complex which does not require any additional expenditures on purchasing and laying a many-kilometer main cable from EC to the coast station as well as on creating or renting this station and its servicing. Thus the cost of the development, fabrication, tests and installation of the autonomous emitting complex in the East Arctic sector has been estimated. The main expenses are due to the development of technical and technological forms and records of the main subsystems and the entire complex, including breadboarding and laboratory tests of its most importants units. Part of the main and auxiliary equipment will be purchased abroad (in the USA). Full-scale (partly full-scale) tests of the complex and its systems should be performed at specially equipped polygons. The complex installation cost for long-term operation is estimated for the shipboard variant.

In the case of deployment from ice involved by the appropriate choice of EC location, the deployment cost including the ice station arrangement can be estimated employing the experience gained in the TAP experiment taking into account the necessary delivery of a larger-size emitting equipment to the station. These costs as well as the expenditures on the emitting complex elevation after one-two year operation are not included in the operation cost. Cost estimate of emitting complex

development and installation is given in Table 12.

Table 12. Cost estimate of emitting complex development and installation.

1. Personnel	$ 180,000
2. Permanent Equipment	$ 25,000
3. Expendable Supplies	$ 100,000
4. Miscelaneous Costs	$ 490,000
5. Travel Expenses	$ 25,000
6. Total Direct Costs	$ 820,000
7. OH & G & A, (10 %)	$ 82,000
8. Total Direct & Indirect Costs	$ 902,000
9. Fee (10 %)	$ 90,200
10. Grand Total	$ 992,200

8. CONCLUSION

The report deals with possible ways of developing a low-frequency emitting complex which is planned to be used in 1996-1997 and later as a basis for step-by-step arrangement of Acoustic Thermometry of the Arctic basin.

1. The design of the complex is elaborated and the requirements to characteristics of its main subsystems are determined on the basis of analyzed peculiarities of the emitting complex employed in the Arctic.

2. The structural schemes of the autonomous moored complex and the complex with electric power supplied by a distant coast station through the main cable have been developed.

3. The operating parameters of the principal subsystems of such emitting complexes are calculated.

4. It has been demonstrated that numerous problems can be solved best by developing an autonomous moored complex. The conditions for reliable functioning of the complex under the conditions of difficult ice situation are provided. Besides, the cost of the development and long-term service of the complex is essentially reduced due to abandoning expensive activities of the main cable installation and the coast station operation.

5. The problems associated with the emitting complex installation are considered. The necessary shipbased facilities have been determined. In the case of required ice development of the complex, the same technology can, in principle, be used based on load-lifting facilities located in the ice station.

6. The suggested autonomous moored emitting complex mounted in the shelf zone 400-600 m deep close to the continental slope in the East Arctic sector (the regions of the Spitsbergen and the Franz Josef Land), will permit to realize in 1996-1997 the first stage of the ACOUS Program at paths of the order of 2600 km during 1-2 years depending on the emission parameters.

7. At the second stage of the ACOUS Program this complex can be used as a basis for developing a complex with deployment depths to 2000 m capable of being located in deep-water Arctic regions.

REFERENCES

1. P.N.Mikhalevsky, A.B.Baggeroer, A.Gavrilov and M.M. Slavinsky. CW and M-sequence transmissions across the Arctic, J. Acoust. Soc. Am., 96, 3235, 1994.

2. P.N.Mikhalevsky, A.B.Baggeroer, A.Gavrilov and M.Slavinsky. Experiment tests use of acoustics to minitor temperature and ice in Arctic ocean. EOS, 1995, v.76, No.27, p.265-269.

3. F.B.Jensen, W.A.Kuperman, M.B.Porter, H.Schmidt. Computational ocean acoustics (American Institute of Physics, New York, 1994).

4. Virovlyansky, A.L. On the temporal structure of pulse signal in underwater sound channel. Akusticheskii Zhurnal, 1985, 31(6): 790-792.

5. D.E.Cartwright. A feasible duty cycle for extracting tide information from ATOC transmissions. ATOC Ocasional Notes, 1994, No 19, p. 1 - 5.

6. M.M.Slavinsky, B.N.Bogolubov. J.L.Spiesberger. Low - frequency sources for ocean acoustic tomography in Full field inversion methods in ocean and seismo-acoustics. Kluwer Academic Publishers, Nethelands, 1995, 217 - 222.

7. M.M.Slavinsky, B.N.Bogolubov. J.L.Spiesberger. (1992). Low - frequency high efficiency sources for acoustic monitoring of climatic temperature changes in ocean basis.J. Acoust. Soc. Am., 92(4),p.p 2349-2350.